ISSN 0016-8521, Geotectonics, 2014, Vol. 48, No. 4, pp. 292–312. © Pleiades Publishing, Inc., 2014.
Original Russian Text © A.A. Fedotova, A.A. Razumovskiy, E.V. Khain, M.O. Anosova, A.V. Orlova, 2014, published in Geotektonika, 2014, Vol. 48, No. 4, pp. 44–66.

Late Neoproterozoic Igneous Complexes of the Western Baikal–Muya Belt: Formation Stages

A. A. Fedotova[a, b], A. A. Razumovskiy[a], E. V. Khain[a], M. O. Anosova[b], and A. V. Orlova[a, c]

[a] *Geological Institute, Russian Academy of Sciences, Pyzhevskii per. 7, Moscow, 119017 Russia*
e-mail: fedotova@ginras.ru

[b] *Institute of Geochemistry and Analytical Chemistry, Russian Academy of Sciences, ul. Kosygina 19, Moscow, 119991 Russia*

[c] *Faculty of Geology, Moscow State University, Moscow, 119234 Russia*

Received March 4, 2013

Abstract—The paper presents new geological, geochemical, and isotopic data on igneous rocks from a thoroughly studied area in the western Baikal–Muya Belt, which is a representative segment of the Neoproterozoic framework of the Siberian Craton. Three rock associations are distinguished in the studied area: granulite–enderbite–charnockite and ultramafic–mafic complexes followed by the latest tonalite–plagiogranite–granite series corresponding to adakite in geochemical characteristics. Tonalites and granites intrude the metamorphic and gabbroic rocks of the Tonky Mys Point, as well as Slyudyanka and Kurlinka intrusions. The tonalites yielded a U–Pb zircon age of 595 ± 5 Ma. The geochronological and geological information indicate that no later than a few tens of Ma after granulite formation they were transferred to the upper lithosphere level. The Sm–Nd isotopic data show that juvenile material occurs in rocks of granitoid series ($\varepsilon_{Nd}(t) = 3.2–7.1$). Ophiolites, island-arc series, eclogites, and molasse sequences have been reviewed as indicators of Neoproterozoic geodynamic settings that existed in the Baikal–Muya Belt. The implications of spatially associated granulites and ultramafic–mafic intrusions, as well as granitoids with adakitic geochemical characteristics for paleogeodynamic reconstructions of the western Baikal–Muya Belt, are discussed together with other structural elements of the Central Asian Belt adjoining the Siberian Platform in the south.

Keywords: Paleoasian ocean, Neoproterozoic, Siberia, Baikal–Muya Belt, adakite, zircon

DOI: 10.1134/S0016852114040049

INTRODUCTION

The Baikal–Muya Belt is situated to the south of the Baikal–Patom Belt (Fig. 1a) in the area with widespread Neoproterozoic carbonate–terrigenous and less abundant volcanic sequences overlying Paleoproterozoic rocks (1.8–2.0 Ga) of the North Baikal Belt of the Siberian Platform margin [15, 31]. The Olokit Zone of intensely deformed rocks and the Synnyr rift structure are localized between two former belts. The Baikal–Muya Belt is divided by a field of Paleozoic granitoids into the western and eastern branches. The western branch consists of three longitudinal zones: two marginal zones of metamorphic rocks, including granulites, and the central zone with predominant Vendian–Cambrian volcanic and carbonate rocks [23]. Granite gneiss of the Muya Block occupies the central part of the eastern branch. Volcanic rocks, sedimentary sequences, and mafic-ultramafic massifs occur in its framework. More detailed schemes of tectonic regionalization of the Baikal–Muya Belt are given in [6, 42, 43]. The Baikal–Vitim Fold System is located to the south of the Baikal–Muya Belt. These structural units are separated by the Baikal Metamorphic Belt, which plays the role of a collisional front [41], or the Barguzin Metamorphic Block [16]. The Baikal–Vitim (Uda–Vitim) Fold System is the late Neoproterozoic–Cambrian suprasubduction belt that arose on the early–middle Neoproterozoic heterogeneous basement [11–13, 33, 40, 41].

In addition to the Late Precambrian rocks widespread in the Baikal Mountains, the Paleozoic, in particular, Middle Paleozoic sequences participate in folding [2, 3, 7, 30]. The age of these rocks is substantiated by geological relationships [4, 5] and paleontological data. The age of final folding has been debated since the first half of the 20th century (Baikalides, early or complete Caledonides?) [4]. New geochronological evidence has not put an end to this discussion. Moreover, new questions arose, as illustrated by two concepts of the Earth's crust formation in the region [43, 44].

The aim of this publication is to integrate the available geological and geochemical information on igneous rocks in the western Baikal–Muya Belt. To solve this problem, we have studied the relationships between mafic and ultramafic rocks, granulites, and granitoids with adakitic geochemical characteristics described in this belt for the first time.

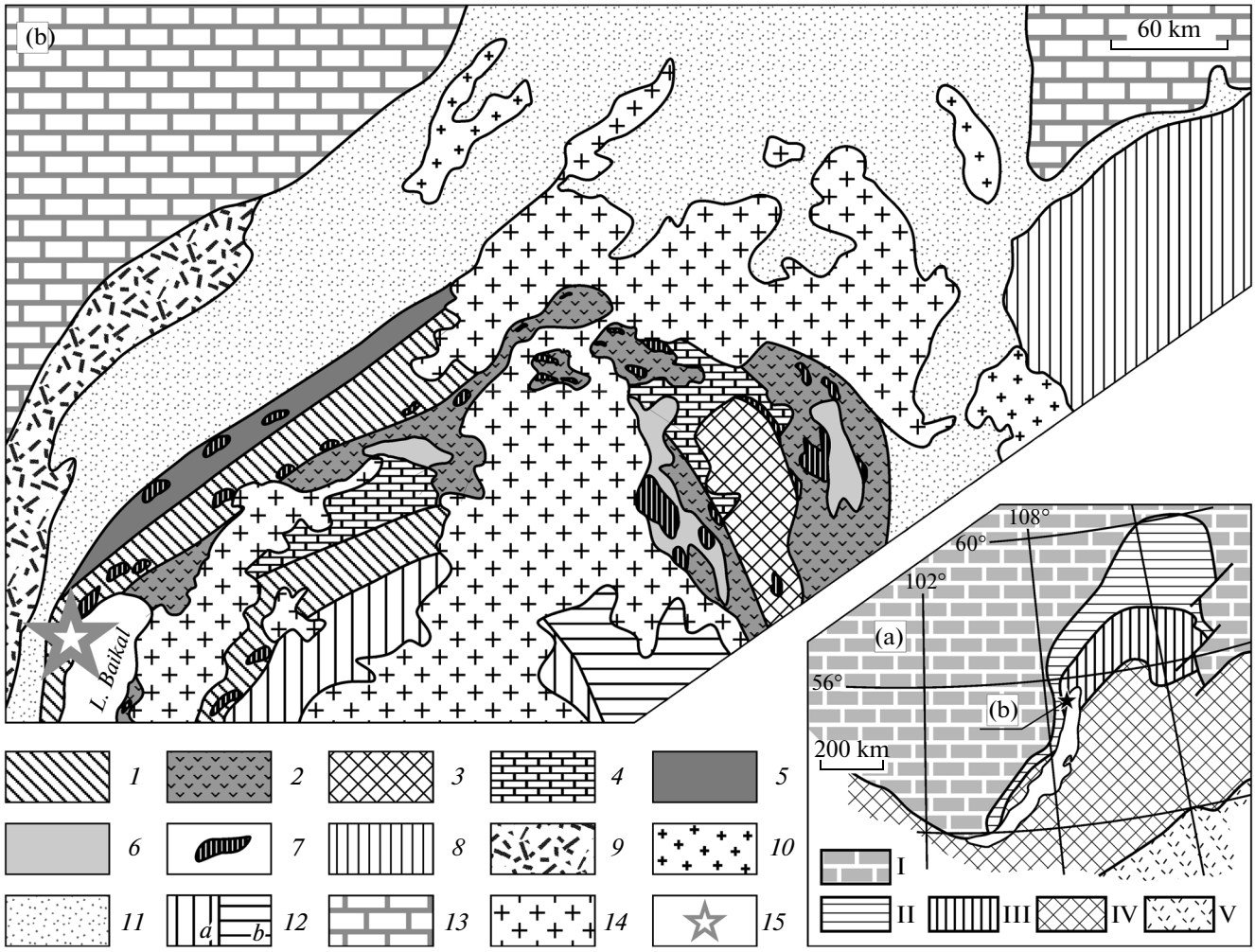

Fig. 1. Position of studied area in (a) tectonic zoning of southern Siberia, after [36, 87] and (b) structure of northern Baikal mountain region, modified after [23]. (I) Siberian Platform; (II) Baikal–Patom Belt: mainly sedimentary and volcanic–sedimentary complexes of Neoproterozoic passive continental margin; (III–V) tectonic collages of rock series in island-arc and continental-marginal arcs and related basins: (III) Neoproterozoic Baikal–Muya Belt, (IV) Late Proterozoic–Early Ordovician Baikal–Vitim (Uda–Vitim) System, (V) Devonian–Mesozoic Mongolia–Okhotsk Belt. (*1–4*) Baikal–Muya Belt: (*1*) Nyurundukan Group: amphibolite, (*2*) Kelyan Group, etc.: metavolcanic rocks, (*3*) Proterozoic (?) metamorphic rocks of the Muya Block, (*4*) Neoproterozoic carbonate sequences; (*5*) Neoproterozoic volcanic–sedimentary complexes of Synnyr Zone; (*6*) Neoproterozoic granitoids of Muya Complex; (*7*) Neoproterozoic mafic–ultramafic massifs; (*8–10*) basement of Siberian Platform: (*8*) Stanovoi Block, (*9*) Akitkan volcanic–plutonic complex; (*10*) granites and gneisses; (*11*) Neoproterozoic Baikal–Patom Belt; (*12*) Kotera Zone: (*a*) mainly sedimentary rocks of Kotera Group; (*b*) volcanic rocks of Gorbylok Formation; (*13*) Neoproterozoic–Paleozoic cover of Siberian Platform; (*14*) Paleozoic granite; (*15*) location of geological scheme 2A.

The results of previously conducted investigations are controversial and often diametrically opposed [1, 23, 28, 29, 43, 45, 54, 64]. The granulite–enderbite complex is mapped along the shore of Lake Baikal as a tract varying in width from less than a few kilometers [23, 29, 54] to a couple of outcrops, e.g., at the southern ending of the Boguchan Bay and Ludar Cape, where they are no more 1 km^2 in total area or they are represented by solitary geological bodies [45]. Metasomatic origin of this complex is assumed [54]. Granitic bodies, which could be reference objects for deciphering the structure, also remain uncertain in scope. For example, the Baikal'sky pluton of the youngest granitoids, shown in several maps and geological schemes [23, 29, 54], is completely ignored in others [1, 64]. In this connection, it is reasonable to discuss new geological data obtained by the authors.

In general, a great body of information on the Baikal–Muya Belt has been gained to date; however, questions concerning its evolution within a time interval from 780 to 650 and about 600 Ma remain open. In the second half of this paper, we propose a new interpretation for the latest events in the belt's history. The indicative role of spatially related granulites and ultramafic–mafic intrusions, as well as of granitoids with adakitic geochemistry, is discussed for this purpose.

NEW GEOLOGICAL DATA AT THE INTERFLUVE OF THE SLUDYANKA AND REL RIVERS

Granulites, charnockites, gneisses, amphibolites, crystalline schists, and ultramafic–mafic bodies occur at the interfluve of the Slyudyanka and Rel rivers (Figs. 3–5). The tonalite–plagiogranite–granite series has been recognized for the first time as an intrusive complex cutting through older rock associations.

The association of crystalline schist, enderbite, and charnockite—high-temperature (800–900°C) and moderate-pressure (8–9 kbar) metamorphic rocks [23, 55]—is traced from Boguchan Bay to the Rel River basin [28, 29]. The metamorphic rocks of the Baikal–Muya Belt combined earlier into the Nyurundukan Formation, or Sequence, but turned out to then be heterogeneous in composition, metamorphic grade, and age [29, 43, 64].

Crystalline schists (two-pyroxene and biotite–pyroxene basic rocks), amphibolite and enderbite (pyroxene–plagioclase rocks), charnockite (pyroxene–two-feldspar rock with antiperthite intergrowths), and products of their retrograde metamorphism (biotite and amphibole–biotite schists and gneisses) are exposed along coastal cliffs of the capes separating Boguchan, Baltakhanov, and Ludar bays; at outcrops on the adjoining highs; and in the Rel River valley, including outskirts of the settlement of Baikal'sky at its mouth (Figs. 2b, 2c). The description of amphibolite and crystalline schist with granulite relics from eastern spurs of the northern Baikal'sky Range near Lake Slyudyansky [23] allows us to refer these rocks to the same complex.

The high-grade metamorphic rocks have deformed into tight folds striking primarily in the northwestern and northern directions (Figs. 2b, 2c). The fold hinges are clearly seen in outcrops with northwestern exposition, in particular, in coastal exposures at the eastern end of Boguchan Bay (Cape Pisany Kamen [64] and the northern part of Cape Ludar). On the upper southern–southeastern slope of the mountain with an 806-m elevation mark to the north of Baikal'sky Settlement (Fig. 2c), fold hinges composed of enderbite or gneiss are emphasized by small elongated ridges. Downslope, fold limbs composed of the same rocks armor outcrops. The crystalline schists are subjected to weathering and fill less exposed depressions. Most likely, this explains the opinion of the occurrence of the large Baikal'sky granitic massif at the left wall of the Rel River valley near its mouth [23, 29, 54, 56].

Thus, basic granulite and charnockite, including intermediate and felsic rocks of normal alkalinity (Figs. 6a, 6b), occur from at least the lower reaches of the Rel River in the south to Boguchan Bay in north (Figs 2b, 2c) and allow us to answer affirmatively whether the granulite complex extends beyond two small sites shown in [1].

The age of 617 ± 5 Ma is the most reliable date obtained with the U–Pb method for individual zircon grains from enderbite exposed on Cape Pisany Kamen [1]. We have sampled enderbites from this cape and gneisses exposed on the southwestern shore of Boguchan Bay (Fig. 7b), i.e., from a peripheral part of the inferred Baikal'sky massif and from its central part. These rocks are divided into two groups by texture and age of zircon and whole-rock Nd model age. Zircons from rocks of the first group crystallized 605–620 Ma ago: enderbite (607 ± 3 Ma), gneiss from Boguchan Bay (608 ± 4 Ma), and charnockite mapped within the Baikal'sky massif (618 ± 4 Ma). The model Nd isotopic age $T_{Nd}(DM)$ of the rocks pertaining to this group is 1.3–0.8 Ga [34, 49]. The rocks of the second group, including enderbite from the central part of the Baikal'sky massif contain zircons dated at 780 Ma and older [35]. Their model Nd isotopic age $T_{Nd}(DM)$ is 2.3–2.2 Ga [34, 49] (Fig. 8). Based on these data, one can preliminarily conclude that basic granulites and charnockites are heterogeneous in initial age, model $T_{Nd}(DM)$ age (2.2–2.3 and 1.3–0.8 Ga), and chemical composition [34, 49].

A complex of amphibolized gabbroic rocks and orthoamphibolites occurs as a small ridge with a 561.3-m elevation mark, which extends from the northwestern shore of Boguchan Bay to the northern shore of Lake Boguchan (Fig. 2b). The complex consists largely of amphibole–feldspar rocks retaining relics of primary gabbroic structure. No biotite-bearing varieties widespread in other areas occupied by metamorphic rocks occur here. Gabbroids in rocky outcrops are medium-grained and, less frequently, coarse- or fine-grained homogeneous rocks; metamorphic banding is occasionally noted. Nonuniform spotty coloration from brown-yellow at the weathered surface of homogeneous fragments to gray-green along fractures is char-

Fig. 2. Geology of western shore of Lake Baikal between Slyudyanka and Ludar bays: (a) index map, (b, c) schematic geological maps of Slyudyanka–Rel interfluve, after V.P. Safronov, A.I. Trepalin, V.I. Smol'kin, et al. (1969) and [23]. (*1*) Quaternary alluvial, proluvial, hillside, lacustrine, glacial, and fluvioglacial sediments, unspecified: clay, loam, sandy loam, sand, pebbles, rubble, cobbles and boulders; (*2*) greenschist, amphibolite, limestone, gneiss of Olokit Zone, unspecified; (*3*) tectonite, mylonite, and blastonylonite; (*4–10*) Neoproterozoic rocks of the Baikal–Muya Belt: (*4*) unspecified, (*5*) two-pyroxene crystalline schist, amphibolite, and amphibolized gabbro; (*6*) leucocratic crystalline schist, enderbite, and charnockite; (*7*) gabbro and amphibole gabbro, (*8*) gabbro, gabbronorite, olivine gabbro, and troctolite; (*9*) amphibolized gabbro, (*10*) granodiorite, leucogranite, and sporadic garnet plagiogranite: bodies (*a*) on scale and (*b*) out of scale; (*11*) faults: (*a*) mapped and (*b*) inferred; (*12*) geological boundaries: (*a*) mapped and (*b*) inferred; (*13*) strike and dip symbols: (*a*) primary (magmatic) mineral banding, (*b*) metamorphic banding, and (*c*) contact of magmatic bodies, mineral flattening and schistosity; (*14*) location of granodiorite–leucogranite samples and their number.

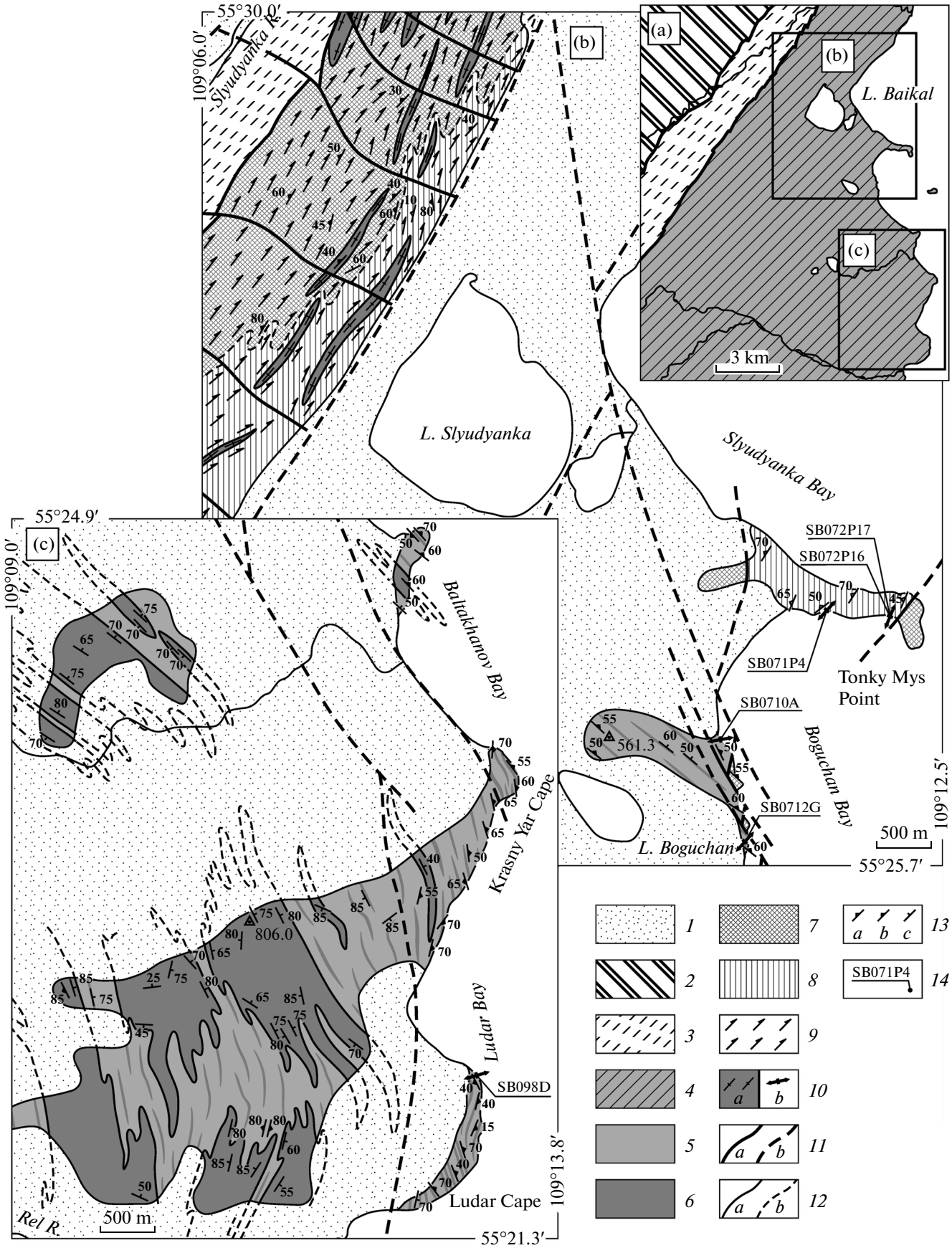
55°30.0′
109°06.0′
Slyudyanka R.
(a)
(b)
(c)
L. Baikal
3 km
L. Slyudyanka
Slyudyanka Bay
SB072P17
SB072P16
SB071P4
Tonky Mys Point
SB0710A
561.3
Boguchan Bay
SB0712G
L. Boguchan
500 m
109°12.5′
55°25.7′
55°24.9′
109°09.0′
Baltakhanov Bay
Krasny Yar Cape
806.0
Ludar Bay
SB098D
Ludar Cape
109°13.8′
Rel R.
500 m
55°21.3′
1
2
3
4
5
6
7
8
9
10
11
12
13
14
SB071P4

acteristic. Melanocratic veins of fine- to medium-grained rocks are observed in gabbroids. Amphibolization obliterates primary relationships; however, it is clear that these veins are 3–15 cm thick; the larger veins have small offsets. In the central and southern parts of the ridge (Fig. 2b), gneiss and amphibolite are exposed as greenish gray amphibole–plagioclase rocks with more pronounced metamorphic rather than magmatic structure. The bodies of gneisses with conformable metamorphic banding (Fig. 7a) are up to 4 m thick and occupy up to 20–25% of the section.

In the southern line of coastal cliffs, monotonic orthoamphibolite members in the most compact parts of outcrops reveal shelly and ball-shaped parting. The size of rounded blocks varies from 3–4 to 20–25 m. The least altered rocks in the central zones of balls are composed of granulite (almost unaltered quartz-bearing two-pyroxene plagioclase rock).

Amphibolized gabbroids and orthoamphibolites with gneiss intrelayers underwent joint deformations. The rocks occur as asymmetric linear folds about 10 m in amplitude with rather steep (50°–65°) metamorphic banding that dips in the northeastern bearings. This indicates a common deformational pattern throughout the metamorphic domain, including the western shore of Boguchan Bay (Figs. 2b, 2c).

Separate blocks of rocks not involved in deformation crop out in cliffs at the western shore of Boguchan Bay. These blocks are apparently juxtaposed with the above-described metamorphic rocks along the left-lateral strike-slip–normal faults (Fig. 2b). These blocks are composed of gabbroic rocks similar to those occurring on Tonky Mys Point (see below). The tectonic contacts of the largest northern block are exposed, and the southern contact is complicated by a transitional zone ~15 m thick, where massive coarse-grained gabbro gives way to banded amphibolized gabbro, which in turn grades into coarse-grained orthoamphibolite.

Amphibolized gabbroic rocks, orthoamphibolites, and quartz-bearing two-pyroxene–plagioclase rocks from western shore of Boguchan Bay are close in composition to one another and to basic crystalline schists of metamorphic complex (Table 1; Figs. 6b, 6c). The minerals of these rocks crystallized in the following succession: olivine, pyroxene, plagioclase, which differs from troctolitic succession in low-Ti rocks of the Tonky Mys layered complex.

The Tonky Mys pyroxenite–troctolite–gabbro complex is exposed most completely as low but almost continuous rocky outcrops along the southern shore (Fig. 3). The substantially gabbroic type of the section (Fig. 4) and alternation of peridotite, pyroxenite, troctolite, and gabbro (Fig. 5) are distinguished.

Peridotite occurs as rare layers of coarse- and giant-crystalline plagioclase-bearing wehrlite 2–15 m in thickness (Fig. 5), as a rule, alternating with clinopyroxenite and websterite. Sporadic dunite lenses (0.5–0.7 m) are noted within peridotite interlayers. Websterite and clinopyroxenite are primarily giant-crystalline rocks (crystals are 1.5 to 4 cm in size). They form layers 5–7 to 15–70 cm thick in thin-banded varieties and 1–10 m in the roughly banded rocks (Fig. 5). Clinopyroxenite layers prevail over websterite layers, which occupy no more than 20% of the total volume. Websterite commonly occurs as separate bands and lenticular segregations (a few decimeters to 2–4 m in thickness) hosted in clinopyroxenite.

Medium- to coarse-grained and less frequent giant-crystalline gabbroic rocks are associated with peridotite and pyroxenite. Coarse-grained troctolite is the most abundant olivine-bearing rock. Olivine is partly replaced with amphibole and/or serpentine; plagioclase occurs as large (0.3–1.5 cm) euhedral crystals. Troctolite interlayers are 2–15 m thick. Gabbro and olivine gabbro are commonly intercalate with clinopyroxenite as interlayers varying in thickness from 2–3 to 15–20 cm in thin-banded varieties and 0.5 to 10–11 m in roughly banded members (Fig. 5). Contacts of olivine gabbro with troctolite and peridotite are less frequent.

The gabbroic type of section in the Tonky Mys layered complex is made up of coarse-grained and giant-crystalline gabbro, olivine gabbro, and probably gabbronorite forming separate interlayers or equant segregations in giant-crystalline and pegmatoid cockarde gabbro. The thickness of these interlayers and segregations varies from 0.5–0.7 to 8.0 m (Fig. 4). Transitional zones decimeters in thickness are clearly seen at the contacts with pegmatoid cockarde gabbro. In addition, amphibole gabbro containing magmatic hornblende (10–60%) plays a substantial role in the gabbroid type of section. This type of gabbro often contains lenses of "gabbro pegmatite" with hornblende crystals up to 15 cm in length. These lenses reached a few meters in extent; their thickness is 30–70 cm. Amphibole gabbro apparently reveals crosscut intrusive relationships with peridodite–pyroxenite–gabbro type of section. The gabbroic type of section is characterized by a gradual transition from gabbro and olivine gabbro, including cockarde varieties, to amphibole gabbro. The transition zone is commonly 1–2 m thick.

The pyroxenite–troctolite–gabbro complex is characterized by magmatic layering, the formation of which was accompanied by viscous–ductile redistribution of material. At the early stage of viscous–ductile deformation, the rocks were transformed into open low-angle folds. This stage is documented by primary mineral banding, which emphasizes the layered character of the complex as a whole. The mineral lineation and flattening are conformable to the dip of limbs in folded mineral banding, and this indicates that both belong to the same deformation stage. At present, the fold system level steeply plunges in the WNW bearings (Fig. 3).

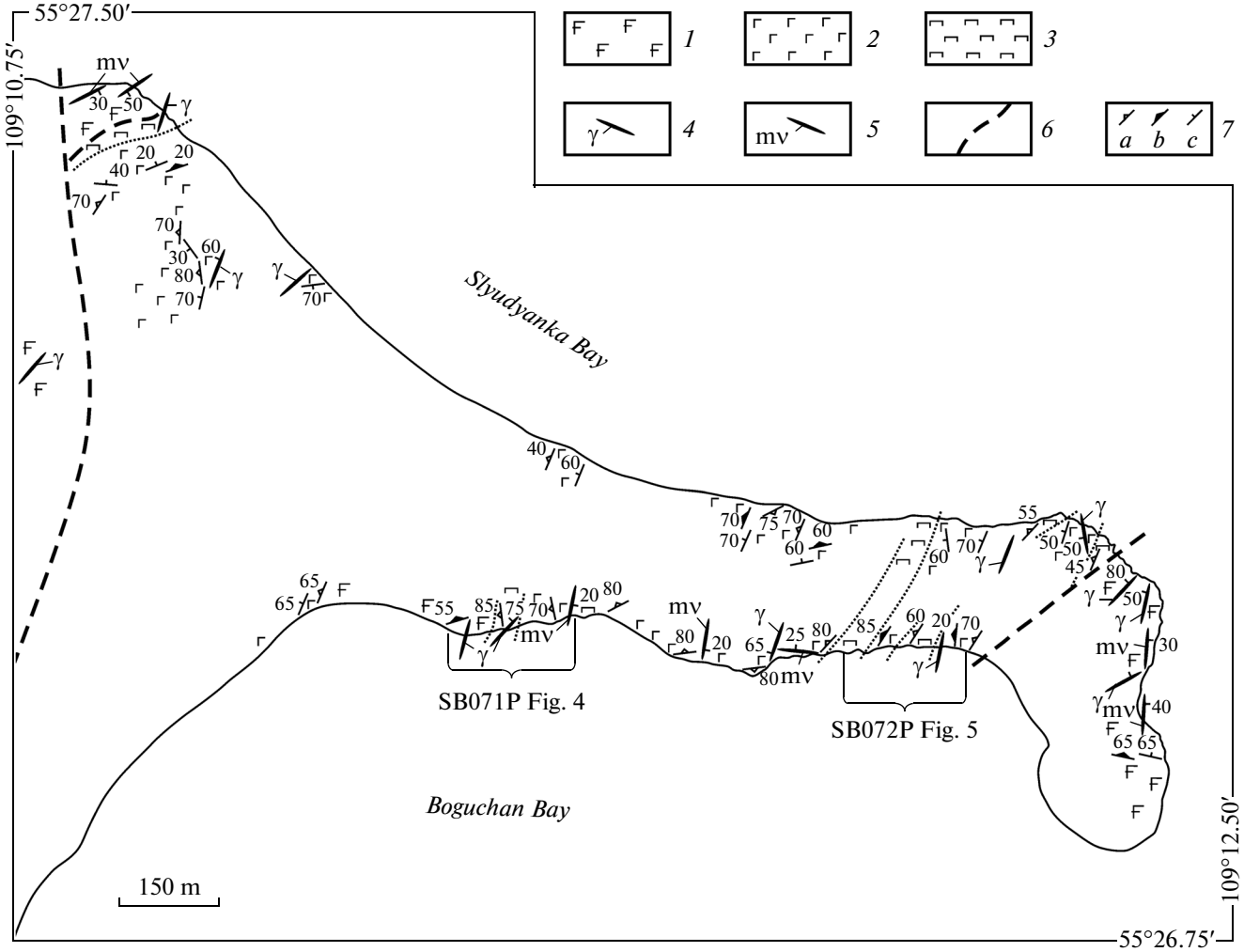

Fig. 3. Geological sketch of Tonky Mys Point. (*1–3*) Areas mostly occupied by bedrock: (*1*) amphibole gabbro, (*2*) gabbro, gabbronorite, troctolite, and olivine gabbro; (*3*) peridotite and pyroxenite; (*4*) dikes: plagiogranite, tonalite, felsite (out of scale); (*5*) melanogabbro dike (out of scale); (*6*) inferred fault; (7) strike and dip symbols: (*a*) primary (magmatic) mineral banding, (*b*) metamorphic banding, and (*c*) contact of magmatic bodies, mineral flattening and schistosity.

The Tonky Mys pyroxenite–troctolite–gabbro complex is characterized by fragments with intensely developed magmatic layering (particular layers are 2–3 to 40–70 cm thick) and by alternating layers from a meter to tens of meters thick composed of massive or schlieren–banded rocks. The thin magmatic (mineralic) banding is mostly caused by variation in the relative amounts of rock-forming minerals. The rough alternation of rocks is complicated by differentiation in grain size. The later metamorphic linear and planar structures (Fig. 3) superimposed upon rocks with already formed mineral banding related to the early stage of deformation are noted over a significant part of the studied area.

Rocks pertaining to the layered complex are nonuniformly altered. Peridotites are markedly serpentinized and pyroxenes are replaced with amphiboles. Clinopyroxenites are partly transformed into serpentine–amphibole schists. The coarse-grained and giant-crystalline gabbroic rocks have the characteristic cockarde structure, when rims around pyroxene crystals are replaced with fine radiaxial amphibole; calcic plagioclase is saussuritized. Magmatic hornblende is mostly replaced with low-temperature green amphibole.

Sporadic melanogabbro dikes cut through the gabbroic portion of the complex and, less frequently, pyroxenites (Figs. 3–5); the eastward (15°–30° E) dip of dikes is persistent; their thickness ranges from 3–5 to 40 cm. The larger bodies are commonly characterized by an inequigranular structure with lenticular, lentil-like segregations of medium- to fine-grained rocks incorporated into the coarse-grained groundmass. Some melanogabbro bodies have distinct chilled contact rims consisting of aphyric and locally develop-

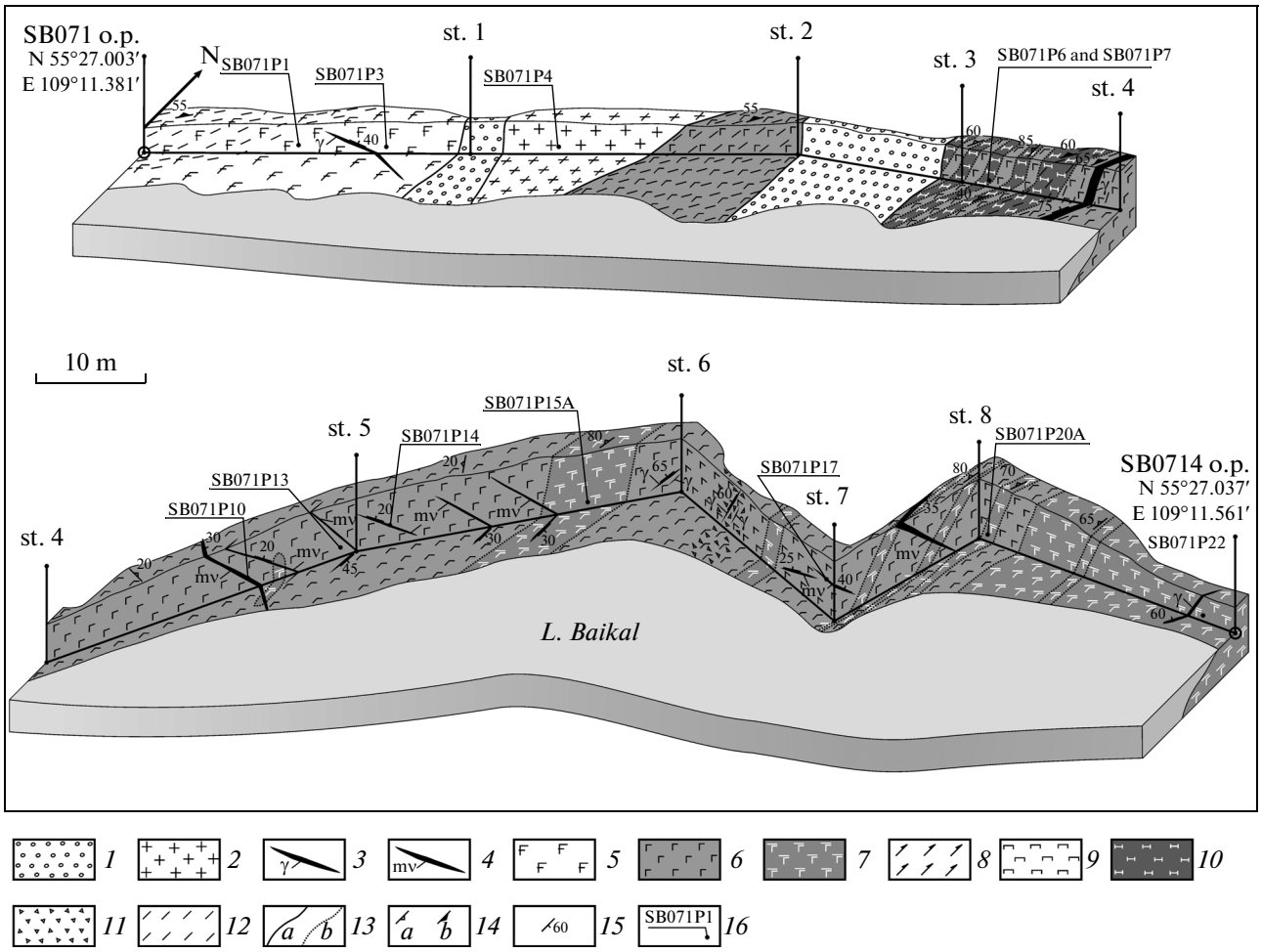

Fig. 4. Geological section SB071P from SB071 to SB0714 o.p. (*1*) Quaternary hillside sediments; (*2, 3*) plagiogranite and less frequent leucoplagiogranite, including garnet-bearing variety; tonalite: (*2*) on scale and (*3*) out of scale; (*4*) melanogabbro dike; (*5*) amphibole gabbro; (*6*) gabbro and gabbronorite; (*7*) troctolite and olivine gabbro; (*8*) amphibolized gabbro; (*9*) peridotite; (*10*) pyroxenite; (*11*) brecciation zone; (*12*) zone of metamorphic schistosity; (*13*) mapped geological boundaries: (*a*) sharp and (*b*) diffuse; (*14*) strike and dip symbols: (*a*) primary (magmatic) mineral banding, (*b*) metamorphic banding; (*15*) strike and dip symbols of magmatic body contact, mineral flattening and schistosity; (*16*) location of samples for chemical analysis and their numbers. o.p., observation point; st, stake.

ing porphyritic rocks with plagioclase phenocrysts and abundant ore mineral in interstices.

Contacts of the Tonky Mys massif are not exposed. The grain size or composition of rocks does not change approaching the boundaries of the area occupied by the pyroxenite–troctolite–gabbro complex. Therefore, this complex is most likely a part of a larger massif or bounded by tectonic contacts.

The rocks making up the Tonky Mys massif are high-Al, owing to the troctolitic sequence of crystallization or special composition of initial melt (Figs. 6c, 6d), and low-Ti (<0.6 wt % TiO_2 except for two samples from the substantially gabbroic type of section) (Table 1). According to the Sm–Nd mineral isochron (olivine, plagioclase, clinopyroxene, whole-rock sample), the age of the Tonky Mys Complex is estimated at 585 ± 22 Ma [29].

The tonalite–plagiogranite–leucogranite complex is represented by a series of hypabyssal intrusive bodies, primarily dikes, which cut through the Tonky Mys pyroxenite–troctolite–gabbro massif, amphibolized gabbroic rocks, alternating crystalline schists and gneisses (Fig. 2). Plagiogranite prevails over tonalite and leucogranite; the latter is distinguished by an extremely low biotite content. Tonalite occurs as thin zones in complexly built bodies (Fig. 7c). Granitoids occur as thin (5–50 cm) dikes and larger intrusive bodies up to 16–18 m thick. Plagiogranite bodies are often complicated by offsets and internal flow structures (Fig. 7c). These bodies, which have intruded into troctolite and gabbro of the Tonky Mys layered com-

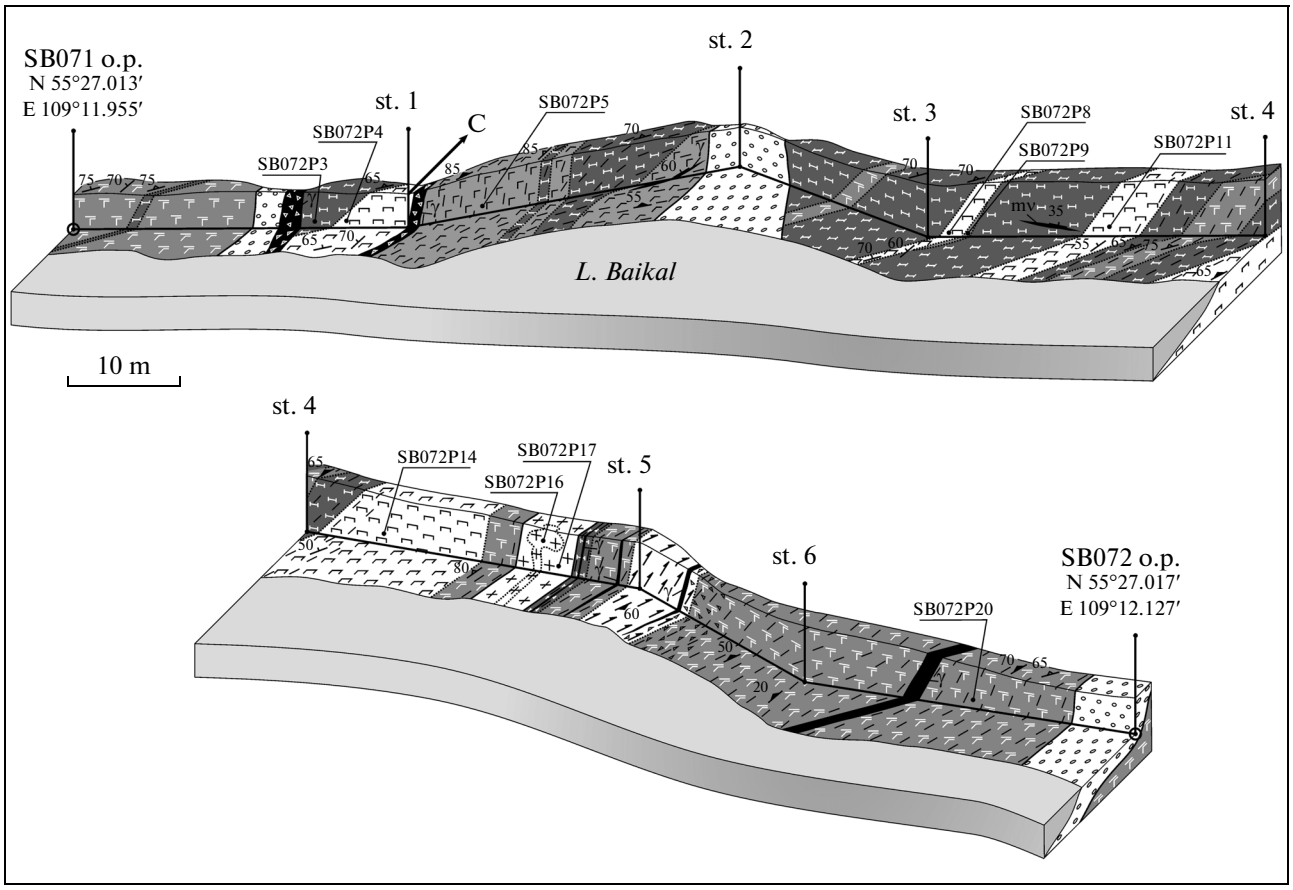

Fig. 5. Fig. 4. Geological section SB072P from SB0716 to SB072 o.p. See Fig. 4 for legend.

plex, are spatially related to zones where gabbroids have been transformed into completely amphibolized rocks. The newly formed planar structural elements, which were the last to be created at a temperature sufficient for penetrative deformation and metamorphism of the layered complex, have been superimposed on mineral banding of the early deformational stage [89]. The plagiogranite bodies, as a rule, intruded along the contacts between rocks differing in competence at limbs of folds emphasized by banding of the layered complex. It should be noted that certain zones of completely amphibolized gabbro tens of meters in thickness do not reveal any spatial links to the exposed granitoid bodies.

The flow structures documented at outcrops are also observed at the microlevel. For example, tonalite sample SB72P17 is a medium-grained crystalline rock consisting of saussuritized plagioclase grains, chloritized biotite flakes, and tabular amphibole crystals incorporated into the fine-grained crystalline allotriomorphic-granular quartz aggregate with a laminar structure. Plagioclase grains have altered selectivity: the advanced saussuritization of cores emphasizes primary zoning. Biotite is almost completely chloritized. Apatite and zircon are accessory minerals.

In the northwestern part of Boguchan Bay, amphibolized gabbro is dissected by a network of granitoid veins and veinlets that apparently formed under conditions of brittle shear failure. Thin veinlets less than 1.0–1.5 cm in thickness are composed of leucogranite. Thicker bodies (0.3–0.6 m) are complicated by numerous offsets. The predominant plagiogranite veins 5–40 cm thick are massive and distinctly intersect the boundaries between gneisses and amphibolized gabbro, as well as metamorphic banding of these rocks.

Plagiogranite in dikes that cut through amphibolites in the western part of Boguchan Bay (sample SB0712G, Fig. 7a) is a rock consisting of large feldspar grains and long-prismatic and acicular amphibole crystals partly or completely replaced with epidote, which are incorporated into the granitic groundmass. The outer zones of feldspar grains occasionally contain quartz ingrowths. The rock has the structure of porphyry. Apatite and zircon are accessory minerals.

Plagiogranite and leucogranite veins cutting through gabbroic rocks of the Slyudyanka massif are distinguished by abundant pegmatoid varieties, including muscovite pegmatites, as well as garnet granite. Sporadic thin (a few meters) bodies of garnet–

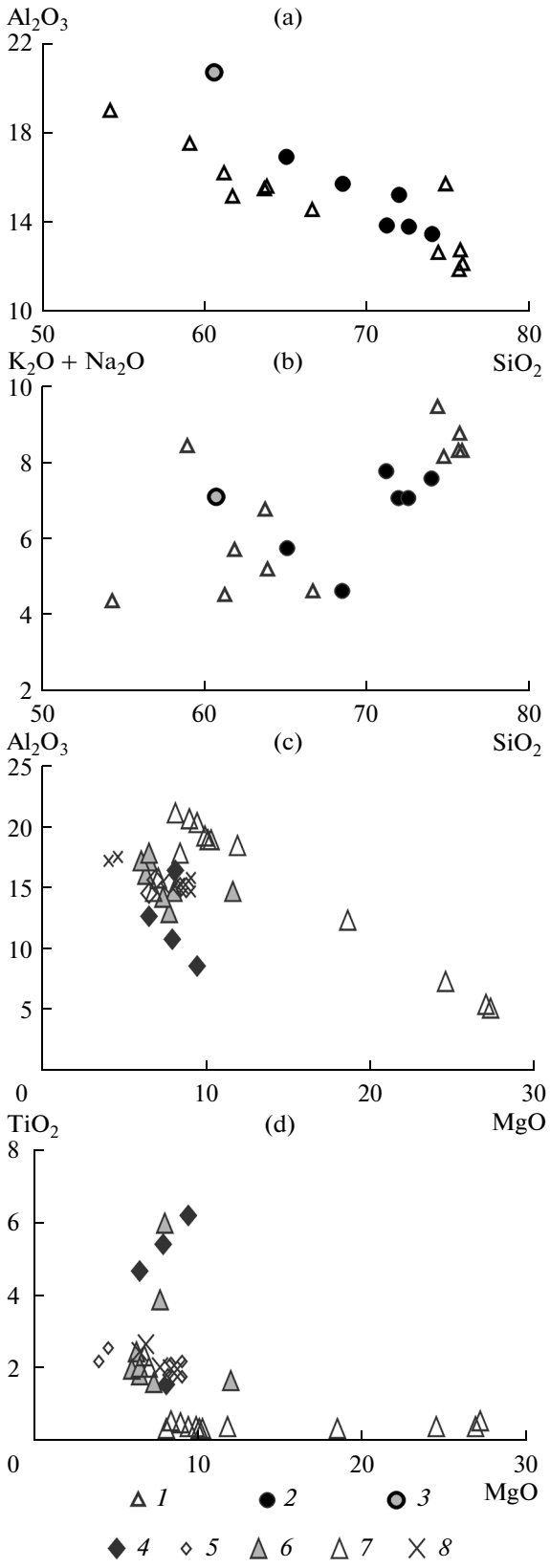

Fig. 6. (a, b) Variation diagrams for subvolcanic granitic bodies, felsic and intermediate rocks of granulite–charnockite complex. (*1*) Gneiss and enderbite, (*2*) granitic rocks of hypabyssal complex, (*3*) high-Al enderbite ($Al_2O_3 > 20\%$). (c, d) Variation diagrams for basic rocks. (*4*) melanocratic microgabbro dikes; (*5*) crystalline schist on Pisany Kamen Point; (*6*) orthoamphibolite and gabbroic rocks in western Boguchan Bay; (*7*) gabbroic rocks of the Tonky Mys massif; (*8*) amphibole crystalline schist in outskirts of Baikal'sky Settlement on Ludar Cape.

amphibole crystalline schists are contained in this massif. Tonalite–plagiogranite–leucogranite veins cutting through the Slyudyanka massif are confined to local shearing and flow zones. Separate plagioclase neoblasts and their clusters are contained in amphibolized gabbro within these zones. The contact between gabbroic and granitoid bodies occasionally acquires a diffuse character. Systems of quartz–feldspar veinlets without sharp contacts chaotically percolate country rocks rather than fill tension cracks. The contact zones between amphibolized gabbroic rocks and granites are locally complicated by low-amplitude flowage and injection folds.

Thus, granitoids injecting the Slyudyanka massif are characterized by joint deformation together with country rocks. This is probably explained by crystallization of granitic rocks at great depth. Granitoids that intrude gabbroic rocks of the Kurlinka massif are closer to the Tonky Mys tonalite–plagiogranite–granite series in composition and morphology of intrusive bodies.

The above data show that the tonalite–plagiogranite–leucogranite complex is not an element of gabbroic massifs. On the contrary, this complex seals the structure formed as a result of juxtaposition of granulite–enderbite–charnockite complex, orthoamphibolites, and related gabbroids of the Slyudyanka and Tonky Mys massifs.

The peculiar magmatic breccia standing out in structure against the background of other rocks in the territory under study is exposed at coastal cliffs of Ludar Cape. The matrix of this breaccia is composed of plagiogneiss. The coarse-grained gabbroic rocks and melanocratic amphibole crystalline schists occur as numerous fragments, which are angular or deformed conformably with gneissic banding of matrix. Along the strike from SW to NNE, the zone of alternating magmatic breccia and gneiss grades into alternation of amphibolite and gneisses. The rocks in coastal zone of Ludar Cape have presumably been included into the metamorphic complex (Fig. 2c), although it cannot be ruled out that they belong to the tonalite–plagiogranite–leucogranite complex.

In geochemistry (Table 2; Figs. 7b, 7d), tonalite and plagiogranite (samples SB072P17, SB0712G) correspond to adakite. These are high-aluminous sodic rocks ($Na_2O > 3.9$ wt %; $K_2O/Na_2O = 0.2$) with Sr content above 400 ppm, low Y (<5 ppm) and HREE contents (in particular, Yb < 1 ppm); the Sr/Y ratio exceeds 90. Leucogranite bodies are referred to this complex on the basis of their structural position. The

dikes (samples SB098D, SB0710A) and the outer zone of the mushroom-shaped tonalite body (sample SB072P16) illustrate such structural links (Figs. 7a, 7b). Leucogranite is distinguished by lower Al_2O_3 content (13.5–15.2 wt %), relatively high Na_2O content (3.3–4.0 wt %), and high $K_2O/Na_2O = 0.7–1.4$. This rock contains less Sr, however Sr/Y ratio remains rather high (>30). The trace element (including REE) contents are similar to other granitic rocks (Table 2; Figs. 7b, 7d). The model $T_{Nd}(DM)$ age of tonalite is 0.7 Ga; $\varepsilon_{Nd}(t) = 7.1$; the model age of three samples ranges of 0.7 to 0.9 Ga; $\varepsilon_{Nd}(t) = 3.2–7.1$ (Table 3; Fig. 8).

Judging by the relationships between the tonalite–plagiogranite–leucogranite complex and gabbroic rocks from the Tonky Mys Point, the latter were not completely cooled crystalline rock during crystallization of granitoids. At the same time, amphibolized gabbro that deformed together with granulites cooled to an extent that assumes brittle failure rather than ductile deformation. The internal flow structures are characteristic of the thickest granitoid bodies in both cases, although such structures did not develop in thin dikes. Plagiogranites and tonalites from two separate bodies (samples SB0712G and SB072P17, see Figs. 2, 7a) intruding into two different complexes coincide in concentrations of trace elements, including REE (Fig. 7e, Table 2).

To estimate the age of the tonalite–plagiogranite–leucogranite complex, samples have been taken from leucogranite of the outer and tonalite of the inner zones of a mushroom-shaped body (Fig. 7b). Individual zircon grains from leucogranite and zircon fraction 0.5 mg in weight from tonalite have been separated. Zircons are represented by similar long-prismatic (acicular) crystals.

The CL images of the internal structure of zircon grains were obtained on a Quanta 200 MK2 SEM equipped with a Gatan add-on device for cathode luminescence study in the wavelength range of 300–1000 nm. It has been established that zircon grains are devoid of alien cores and characterized by fine oscillatory zoning typical of crystallization from magma. This makes it possible to use laser ablation for isotopic dating. Isotopic LA ICP-MS analysis has been carried out for 42 zircon grains on a high-resolution Element-XR mass spectrometer at the Laboratory of Isotopic Geochemistry and Geochronology, Institute of Geochemistry and Analytical Chemistry, Russian Academy of Sciences; the analytical technique was described in [24, 25]. A New Wave Research UP-213 laser was applied. The measurement parameters are as follows: crater diameter 30–40 μm, frequency of laser radiation pulses 4 Hz. The experimental data were processed using the Glitter [92] and ISOPLOT [84] programs. All uncertainties are given at a 2σ level.

The results of U–Pb isotopic analysis of 42 zircon grains from sample SB072P17 (Table 4; Fig. 9) yielded a discordia line whose upper intersection with concordia corresponds to 595 ± 5 Ma and the lower intersection is close to zero (MSWD = 1.2). These data indicate that no metamorphic impact with loss of radiogenic lead by zircon took place in the geological history of this rock. The date at 595 ± 5 Ma is interpreted as the age of magmatic zircon from tonalite.

As judged from published geochemical data [23], granitoids with adakitic characteristics also occur beyond the Slyudyanka–Rel interfluve, where they are exposed as a number of plutons.

ROCK ASSOCIATIONS AS INDICATORS OF THE GEOLOGICAL EVOLUTION OF THE BAIKAL–MUYA BELT

The island-arc volcanic and plutonic rocks are related to one of early stages in the evolution of the Baikal–Muya Belt from U–Pb and Sm–Nd isotopic data [18, 42, 43]. These data imply that island-arc structures whose relics are incorporated into the belt existed 830–800 ago. Older island-arc complexes have been characterized more completely in eastern segment of the belt, where the Kelyan island arc has been reconstructed [5]. The origin of ultramafic–mafic complexes dated at 735–585 Ma remains a matter of debate, and the question on nature of this stage is still open.

The next epoch related to subduction is also based on evidence from the eastern Muya–Baikal Belt, where gabbroic rocks of the Zaoblachny massif are dated at 612 ± 62 Ma and the age of eclogite pertaining to the North Muya Complex is 653 ± 21 Ma [58]. Other geodynamic settings have also been reconstructed for the period of 650–600 Ma: continental rifting for the eastern Baikal–Muya Belt [5] and collision throughout the belt as a whole [54].

Ophiolites conventionally recognized in the inner zone of Baikalides [46] pertain ing to the Baikal–Muya Belt served as a reference complex [5, 22, 69]. However, detailed study of the massifs including into the ophiolitic belt has shown that its scope is disputable [8, 17, 18, 20, 21, 29, 54, 57, 59, 69]. It cannot be ruled out that there are no ophiolites in the Baikal–Muya Belt at all [42]. Thus, the question remains open.

Granulites, as rocks of high-temperature and moderate pressure (up to 8–9 kbar) [23, 55], are widespread in the near-shore part of the western Baikal–Muya Belt. The geodynamic setting of granulite formation is also debatable. The following conditions are suggested: deep levels of the oceanic plateau, backarc zones of island-arc systems, and deep levels of the orogenic plateau similar to Tibet [62, 63]. According to Ellis [76], granulites either ascend during the next orogenic cycle after their formation or their residence time at deep crustal levels measures tens of million years.

In our case, the resolving capability of the performed geochronological study is sufficient to show

SB0712 o.p.
N 55°25.825′
E 109°10.838′
SB0712G
SB0712A
SB0712V
30 cm
(a)
SB072 o.p.
N 55°26.985′
E 109°12.112′
SB072P16
SB072P17
40 cm
(b)
Enderbite gneiss
High-Al enderbite
(c)
Enderbite gneiss
Adakite
(d)
(e)
Rock/chondrite
Rock/primitive mantle
La Ce Pr Nd Sm Eu Gd Tb Dy Ho Er Tm Yb Lu
Rb Th Nb Ce Nd Zr Sm Ti Dy Er Lu
Ba U La Sr Sm Hf Eu Gd Y Yb
1
2
3
4
5
6
7
8
9
10
11
12
13
14
15
16
17

Fig. 7. Relationships of granitoids with: (a) amphibolite and gneiss in western Boguchan Bay (SB0712 o.p.) and (b) gabbroic rocks on Tonky Mys Point (SB072 o.p.); (c, d) chondrite-normalized REE patterns of gabbroic rocks, amphibolites, granulites, and granitoids; (e) primitive mantle-normalized spidergram for granitic rocks of hypabyssal complex; the basis of normalization was taked from [47] and [60], respectively. (*1*) Talus; (*2*) orthoamphibolite; (*3*) gneiss; (*4*) amphibolized olivine gabbro; (*5*) amphibolized pyroxenite; (*6*) leucogranite; (*7*) tonalite and plagiogranite; (*8*) faults: (*a*) proved and (*b*) inferred; (*9*) geological boundaries: (*a*) proved and (*b*) inferred; (*10*) strike and slip symbols for contacts of magmatic bodies, mineral flattening, and schistosity; (*11*) location of samples and their numbers; (*12–17*) legend to graphs: (*12*) orthoamphibolite SB0712A, (*13*) gneiss SB0712V, (*14*) plagiogranite dike SB0712D, (*15, 16*) leucogranite and tonalite SB072P16 and SB072P17, respectively; (*17*) leucogranite dike SB098B (location of sample is shown in Fig. 2c). Average values for enderbite gneiss for the studied area, high-Al enderbite gneiss SB094B from Pisany Kamen Cape, and high-silicic adakite (HSA), after [86], are shown.

that the time interval between the formation of granulites and their transport to the upper crustal level does not measure hundreds of million years and that granulites were formed and exhumed during the same tectonic cycle. Thus, the settings of continent-continent collision should be ruled out from the above-listed paleodynamic settings of the formation and exhumation of granulites in western Baikal–Muya Belt. The model Nd age of the granulite complex at 2.2–2.3 Ga (Fig. 8) eliminates the oceanic plateau setting. Thus, of the three listed settings, only conditions of backarc regions can be chosen. Further, we discuss whether the conditions of granulite formation at active continental margins are constrained only by backarc areas or should other extension situations against the background of shortening be taken into account.

Ultramafic–mafic complexes related to granulites are known in the Alpine–Himalayan and Pacific mobile belts [32 and references therein]. The granulites proper form under a wide range of tectonic conditions, but their spatial relationship with ultramafic–mafic rocks is apparently controlled by a more specific situation. In our opinion, this situation is determined by the existence of asthenopheric windows beneath continental margins.

The most favorable setting for the appearance of asthenospheric windows arises at the continental margin in the case when a spreading range plunges beneath the continental margin. The axial rift of this ridge is a weakened zone facilitating slab breakoff and breakup of the subducting lithosphere. At present, this mechanism is realized at the eastern Pacific margin, where active spreading ridges—Juan de Fuca in California [67, 83] and South Chile in South America [72, 82]—are involved in subduction. A similar situation is observed in the southern Papua New Guinea Archipelago and on the D'Entrecasteoux Islands [61, 75]. This phenomenon in the above region is accompanied by obduction of ophiolites over the continental margin, intense contrasting magmatic activity, and metamorphism, on the one hand, and intrusion of mantle-derived melts along with emplacement of abundant granitoid plutons, on the other hand. The obduction of ophiolites leads to thickening of the crust from above owing to the stacking of allochthonous sheets. Uplift and extension after obduction of ophiolites lead to fast exhumation of igneous and metamorphic rocks (granulites and eclogites), which originated at great depth. Their ascent and exhumation is closely related to entrainment by anomalously heated mantle emerging from the asthenospheric window [52].

The subduction of the spreading ridge beneath the active continental margin has been reconstructed for the Cenozoic margin of Alaska [73], the Ordovician stage in the evolution of the Northern Appalachians [90], western Mongolia and the Eastern Sayan [50–53].

In contrast to situations related to subduction of active ocean ridges (active oceanic windows), other theoretically possible geodynamic settings are also possible. Subducting slab breakoff as a result of subduction zone wedging with simultaneous plunging of the frontal, partially or completely eclogitized slab can be called a *passive asthenospheric window* [38]. The window in the subducting oceanic crust (the absence of a subducting slab and powerful mantle plume (spreading range)) results in a rise in isotherms due to the gap in the screening effect of slab. When the thickness of the lithospheric block that has wedged subduction zone is sufficient, the process can cease with uplift and erosion of the territory.

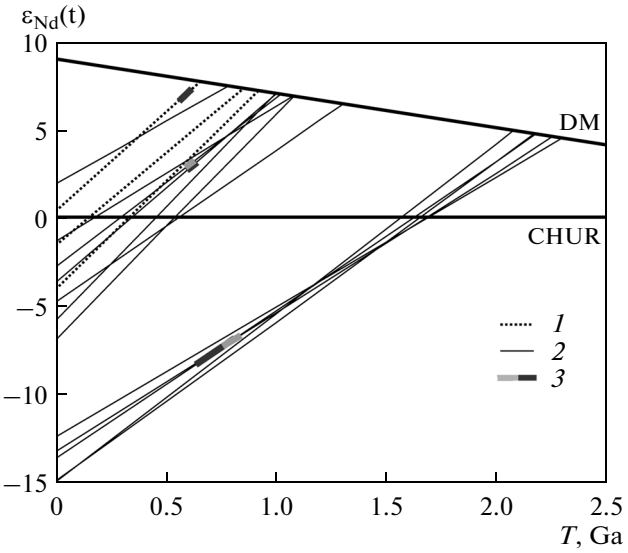

Fig. 8. Evolution lines of Nd isotopic composition of rocks pertaining to granulite–enderbite–charnockite complex and granitoids from crosscutting bodies. (*1*) Enderbite–granulite complex, (*2*) granitic rocks, (*3*) range of U–Pb zircon age [34, 35].

Table 1. Chemical compositions (major oxides, wt %) of ultramafic and mafic rocks from Tonky Mys Point and western Boguchan Bay

No.	Sample	SiO_2	TiO_2	Al_2O_3	Fe_2O_3	FeO	MnO	MgO	CaO	Na_2O	K_2O	P_2O_5	LOI	Total
1	SB071P1	45.89	2.35	14.82	5.16	6.65	0.15	6.83	13.98	2.20	0.18	0.09	1.91	100.21
2	SB071P3	46.21	2.04	15.91	4.95	5.48	0.14	7.08	14.34	2.27	0.19	0.08	1.22	99.91
3	SB071P6	47.43	0.58	17.99	3.93	3.45	0.10	8.41	11.64	3.26	0.20	0.08	2.14	99.21
4	SB071P7	39.53	0.39	12.45	5.39	8.39	0.18	18.58	9.15	0.98	0.14	0.08	4.03	99.29
5	SB071P13	44.79	0.38	18.96	3.68	5.90	0.13	10.10	10.08	3.00	0.17	0.11	2.04	99.34
6	SB071P15A	45.33	0.36	19.02	3.88	6.82	0.15	10.31	9.44	2.74	0.16	0.06	1.04	99.31
7	SB071P20A	45.40	0.43	19.34	2.63	7.61	0.14	9.89	10.30	2.88	0.15	0.05	0.41	99.23
8	SB071P22	47.37	0.35	21.16	4.59	2.80	0.10	8.08	10.22	3.20	0.37	0.10	1.82	100.16
9	SB072P3	37.06	0.32	8.13	9.51	6.63	0.22	25.29	3.03	0.21	0.04	0.06	9.23	99.73
10	SB072P4	38.02	0.44	7.32	12.06	6.26	0.24	24.57	4.38	1.04	0.22	0.09	5.66	100.30
11	SB072P5	46.35	0.51	20.77	2.96	5.51	0.11	8.99	9.04	3.46	0.38	0.09	2.45	100.61
12	SB072P8	34.66	0.42	5.47	14.04	8.53	0.27	26.97	3.23	0.92	0.07	0.09	5.82	100.49
13	SB072P9	46.06	0.42	20.38	4.41	5.03	0.13	9.41	9.09	3.07	0.22	0.08	0.95	99.24
14	SB072P11	35.73	0.58	5.17	13.46	10.12	0.30	27.24	3.98	0.96	0.07	0.08	3.23	100.94
15	SB072P14	37.61	0.48	7.50	10.92	6.31	0.20	25.24	3.69	0.91	0.24	0.08	7.60	100.78
16	SB072P20	44.39	0.43	18.62	4.21	6.19	0.14	11.88	9.06	2.48	0.26	0.08	1.84	99.58
17	SB0711V	44.20	5.95	14.80	1.19	10.00	0.16	8.00	10.20	2.73	0.24	0.08	2.17	99.72
18	SB0711G	44.20	3.88	13.00	3.10	9.87	0.24	7.70	12.00	1.58	0.28	0.92	3.37	100.14
19	SB0711D	47.80	1.62	14.33	5.72	6.28	0.16	7.35	9.53	3.21	0.59	0.31	2.70	99.60
20	SB0711Zh	44.20	2.45	16.14	6.32	8.02	0.14	6.31	11.60	2.85	0.26	0.07	1.13	99.49
21	SB0712E	47.65	1.98	17.31	6.16	4.66	0.16	6.00	10.78	2.94	0.75	0.43	0.97	99.79
22	SB0712Zh	44.65	1.65	14.74	6.61	6.98	0.18	11.65	10.00	2.10	0.62	0.24	0.54	99.96
23	SB0713B	47.16	2.04	17.88	4.20	6.45	0.17	6.47	10.82	3.33	0.42	0.40	0.27	99.61
24	SB0711A	46.46	1.56	16.58	5.25	6.27	0.15	8.13	11.83	2.57	0.21	0.08	0.84	99.93
25	SB071P10	40.69	4.66	12.73	6.74	12.25	0.23	6.51	10.72	2.45	0.19	0.91	1.08	99.16
26	SB071P14	35.36	5.41	10.87	6.20	12.53	0.27	7.92	12.68	1.76	0.14	4.58	2.25	99.97
27	SB071P17	35.51	6.19	8.67	6.36	14.03	0.31	9.47	12.67	1.68	0.18	3.15	1.35	99.57

Rocks: (1–16) layered complex and (25–27) crosscutting dikes from Tonky Mys Point; (20, 24) similar gabbroic rocks and (17) crosscutting dikes from tectonic block in western Boguchan Bay; (18, 19, 21, 22) amphibolized gabbro, orthoamphibolite, and (23) granulite in central zone of fragments with ball-shaped parting from western Boguchan Bay. The location of samples at Tonky Mys Point is shown in Figs. 4 and 5.

The complex of granitoids with adakitic geochemistry turned out to be a new indicator that characterizes the geological evolution of the northern Baikal region. A dike complex composed of tonalitie, trondhjemite, and granodiorite comparable with adakites in geochemistry occurs at the interfluve of the Slyudyanka and Rel rivers. The origin of these rocks is related to partial melting of mafic material [65, 68, 70, 85, 86]. Their key isotopic characteristics—high Sr and LREE contents along with low HREE and Y concentrations—are evidence for melting that leaves behind eclogite or garnet peridotite as restite. The mafic source is considered to be material of the lithospheric mantle plunging into subduction zone [68, 70] or the lower part of the thickened crust [93]. One possible scenario for the formation of granitoids with adakitic parameters is related to melting at the margin of the lithospheric window [68].

The low MgO and Nb contents in granitoids with adakitic characteristics can be explained by the subduction-related setting and melting of the subducting lithosphere contemporaneously with injection of granitoid dikes 595 ± 5 Ma ago. At the same time, there are no sufficient grounds to rule out melting of the lower crust or to deny a mixing mechanism.

Neoproterozoic molasse is one more reference rock complex indicating that the Baikal–Muya and Baikal–Patom belts underwent folding and erosion in the late Neoproterozoic. The Kholodnaya River formation in the Olokit Zone, the Padrokan formation in

Table 2. Chemical compositions (major oxides, wt %; trace elements, ppm) of granitoids and country metamorphic rocks (observation point SB0712) at shores of Boguchan and Ludar bays

Component, %	SB0712A	SB0712V	SB0712G	SB0710	SB071P4	SB072P16	SB072P17	SB098D	SB094B
	SB0712 o.p.			granitoids of hypabyssal complex					enderbite
SiO_2	47.22	75.64	68.44	71.90	72.49	73.91	65.01	71.15	60.68
TiO_2	1.84	0.28	0.38	0.18	0.20	0.15	0.43	0.34	0.40
Al_2O_3	17.22	12.75	15.70	15.24	13.82	13.50	16.90	13.87	20.62
Fe_2O_3	4.28	1.22	2.44	1.12	1.67	0.70	1.24	1.66	3.02
FeO	6.49	0.31	0.72	0.50	0.24	0.15	1.66	1.04	1.04
MnO	0.18	0.02	0.04	0.03	0.06	0.03	0.05	0.03	0.07
MgO	6.49	0.40	1.69	0.68	0.60	0.80	2.55	1.06	0.89
CaO	11.09	0.53	5.16	2.80	2.11	1.93	5.03	2.45	5.67
Na_2O	3.28	3.48	3.90	4.25	4.21	4.03	4.76	3.26	5.62
K_2O	0.54	5.24	0.71	2.79	2.82	3.53	0.98	4.49	1.47
P_2O_5	0.41	0.04	0.10	0.06	0.07	0.07	0.15	0.09	0.17
LOI	0.44	0.34	0.65	0.40	0.74	0.35	1.06	0.46	0.25
Total	99.48	100.25	99.92	99.94	99.03	99.15	99.82	99.89	99.89
V	246	11.6	36.4	–	–	5.79	40.1	24.9	32.1
Cr	158	32.4	24.8	–	–	41.4	42.8	34.6	29.1
Mn	1268	165	236	–	–	216	331	201	467
Co	46.4	1.99	6.76	–	–	1.22	9.49	4.16	6.1
Zn	78	22.9	32.7	–	–	12.2	44.4	24.7	43.3
Ga	19.9	18.1	17.8	–	–	15.1	18.2	13.1	25.8
Rb	3.4	107	10.3	–	–	23.9	11.8	68.5	5.35
Sr	542	43.5	398	–	–	265	582	337	724
Y	29.2	25.4	4.36	–	–	6.83	4.28	6.41	6.9
Zr	186	157	64.7	–	–	26.3	63.8	161	335
Nb	7.2	4.16	1.25	–	–	2.55	1.77	2.05	2.31
Cs	0.02	0.11	0.23	–	–	0.19	0.07	0.35	0.44
Ba	198	310	191	–	–	1116	309	1285	520
La	17.4	26.8	9.23	–	–	4.16	8.57	14.1	20.5
Ce	41.7	58.1	17.3	–	–	8.65	17.8	44.5	32.9
Pr	5.58	6.95	2.03	–	–	0.93	1.99	2.73	3.42
Nd	24.7	26.1	7.71	–	–	3.56	7.68	8.87	12.1
Sm	5.63	5.3	1.45	–	–	0.86	1.54	1.51	1.97
Eu	1.75	0.64	0.45	–	–	0.43	0.56	0.58	2.6
Gd	5.78	4.81	1.15	–	–	0.88	1.26	1.25	1.59
Tb	0.92	0.80	0.16	–	–	0.17	0.16	0.19	0.22
Dy	5.66	4.85	0.84	–	–	1.08	0.87	1.06	1.28
Ho	1.18	1.01	0.17	–	–	0.24	0.1	0.24	0.28
Er	3.17	2.82	0.42	–	–	0.71	0.43	0.82	0.83
Tm	0.46	0.41	0.06	–	–	0.13	0.06	0.14	0.13
Yb	2.88	2.48	0.40	–	–	0.88	0.42	0.99	0.88
Lu	0.44	0.35	0.07	–	–	0.15	0.07	0.19	0.16
Hf	3.66	4.03	1.36	–	–	0.90	1.52	3.39	6.06
Ta	0.58	0.96	0.20	–	–	0.81	0.32	0.15	0.20
Th	0.28	3.79	1.21	–	–	0.84	1.09	8.95	0.36
U	0.08	1.03	0.31	–	–	0.30	0.39	0.86	0.25

SB0712A, melanocratic crystalline schist; SB0712V, gness; SB0712G, plagiogranite, see Fig. 7a; tonalite, plagiogranite, leucogranite, see Fig. 2; SB094B, aluminous enderbite from Pisany Kamen Point; dash denotes not analyzed.

Table 3. Rb–Sr and Sm–Nd isotopic data for granitoids of hypabyssal complex from Slyudyanka–Rel interfluve

Sample	Content, ppm		Isotope ratio			$\varepsilon_{Sr}(t)$	Content, ppm		Isotope ratio			$\varepsilon_{Nd}(t)$	$T_{Nd}(DM)$
	Rb	Sr	$^{87}Rb/^{86}Sr$	$^{87}Sr/^{86}Sr$	$\pm 2\sigma$		Sm	Nd	$^{147}Sm/^{144}Nd$	$^{143}Nd/^{144}Nd$	$\pm 2\sigma$		
SB072P17	10.8	586	0.0532	0.70338	0.00001	−22.5	1.72	9.50	0.1093	0.512643	0.000017	7.1 ± 0.3	0.74
SB098D	71.0	344	0.5964	0.70830	0.00001	−17.2	1.42	8.51	0.1013	0.512414	0.000009	3.2 ± 0.2	1.00
SB0712G	9.97	457	0.0631	0.70340	0.00002	−22.1	0.92	4.82	0.1153	0.512556	0.000013	4.7 ± 0.2	0.94

Model parameters. Mantle uniform reservoir (UR): $^{87}Sr/^{86}Sr = 0.7045$, $^{87}Rb/^{86}Sr = 0.01039$; chondrite uniform reservoir (CHUR): $^{143}Nd/^{144}Nd = 0.512638$, $^{147}Sm/^{144}Nd = 0.1967$; mantle depleted reservoir (DM): $^{143}Nd/^{144}Nd = 0.513151$, $^{147}Sm/^{144}Nd = 0.212$. Analytical studies have been carried out at the Institute of Geochemistry and Analytical Chemistry, Russian Academy of Sciences, using standard techniques [37].

the eastern branch of the Baikal–Muya Belt, the Anagra and Dogaldyn formations in the Bodaibo district consist of sandstone, gravelstone, and conglomerate with fragments derived from proximal provenances. The stratigrahic correlation of these sequences indicates that the Baikal–Muya Mobile Belt and the shelf region of the Baikal–Patom Belt were conjugate elements in the lateral series that jointly underwent mountain building in the Neoproterozoic.

A similar lateral series is illustrated by the recent northern shelf of Australia converging in the Miocene–Pliocene with the island-arc system of the southern Indonesian region, where wedging of the subduction zone by the continental margin results in destruction of the slab plunging beneath the Sunda–Banda arc [66, 71, 74, 77, 78, 91]. Differential movements with a strike-slip component occur under these conditions over a relatively short time span.

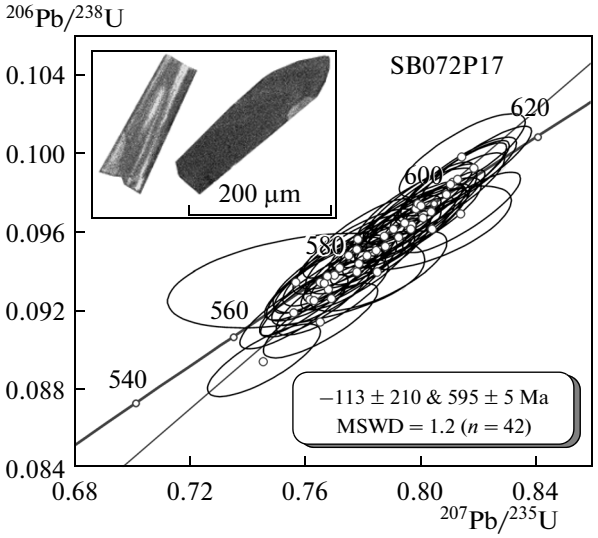

Fig. 9. Concordia diagram for zircons from sample SB072P17 with CL images of typical zircons.

Neoproterozoic erosion and mafic magmatism were also noted earlier in the North Baikal region, where these processes were explained by superimposed rifting [5, 54]. Granulites, gabbroic plutons, and adakites in the western Baikal–Muya Belt formed over a short time interval; deep-seated rocks were transported to upper levels of the lithosphere instantaneously in geological comprehension. Granitoids sealed the heterogeneous structure no later than a few million years after the formation of granulites. Such a geological situation is related, in our opinion, to the passive asthenospheric window beneath the continental margin. This mechanism explains the supply of heat necessary for granulite–charnockite complex formation, juxtaposition of different in age rock complexes in the course of intense tectonic movements, and ascent of mantle-derived magmas providing emplacement of plutons at various depths. In the western Baikal–Muya Belt, these are the Tonky Mys gabbroic complex and the Slyudyanka and Kurlinka massifs. The broken-off subsiding plate leads to decompression, which in turn gives rise to variously oriented tectonic movements, transportation of granulites into the upper crust, emplacement of granitoids with adakitic geochemistry, and formation of backarc basins filled with coarse-clastic mollase.

DISCUSSION

The published information on the northern Baikal region, including the Baikal–Muya Belt as a whole, and other regions makes it possible to consider the relationships between this belt and other structural elements in the southern and southeastern framework of the Siberian Platform (Fig. 10). An oceanic basin and one or several subduction zones variable in age existed in the early Neoproterozoic or at the end of Mesoproterozoic [12, 27, 33, 48, 79]. The evolved volcanic arcs that arose since ~830 Ma ago are represented by their roots in the Muya segment of the belt [17, 18], in the Ol'khon region [10], and have been retained as suprasubduction volcanic series in the eastern Sayan and western Mongolia (Sarkhoi and Darkhat

Table 4. Results of U–Pb isotopic analysis (LA ICP-MS) of zircons from tonalite (sample SB072P17)

No.	Point	Concentration		Th/U	Isotope ratio						Rho	Age, Ma		D
		Th, ppm	U, ppm		$^{207}Pb/^{206}Pb$	±%	$^{207}Pb/^{235}U$	±%	$^{206}Pb/^{238}U$	±%		$^{206}Pb/^{238}U$	±%	
1	2P17-03	46	137	0.33	0.0598	2.5	0.7821	2.2	0.0949	1.7	0.76	584.4	1.6	–0.4
2	2P17-04	1192	938	1.27	0.0597	2.2	0.7625	1.9	0.0927	1.7	0.89	571.3	1.6	–0.7
3	2P17-05	595	612	0.97	0.0607	2.4	0.7658	2.1	0.0915	1.7	0.80	564.6	1.6	–2.2
4	2P17-06	49	272	0.18	0.0596	2.4	0.7993	2.1	0.0973	1.7	0.80	598.4	1.6	0.3
5	2P17-09	50	138	0.36	0.0595	2.6	0.7708	2.3	0.0939	1.7	0.75	578.6	1.6	–0.3
6	2P17-14	447	461	0.97	0.0599	2.3	0.7970	2.0	0.0965	1.7	0.85	593.7	1.6	–0.3
7	2P17-19	691	731	0.95	0.0597	2.3	0.7566	2.0	0.0920	1.7	0.83	567.3	1.6	–0.8
8	2P17-21	413	496	0.83	0.0601	2.4	0.8016	2.0	0.0968	1.7	0.82	595.7	1.6	–0.3
9	2P17-23	512	580	0.88	0.0598	2.4	0.7640	2.1	0.0926	1.7	0.81	571.0	1.6	–0.9
10	2P17-29	1433	970	1.48	0.0605	2.4	0.7461	2.1	0.0895	1.7	0.79	552.7	1.6	–2.4
11	2P17-30	661	649	1.02	0.0599	2.3	0.7855	2.0	0.0952	1.7	0.85	586.0	1.6	–0.4
12	2P17-32	543	556	0.98	0.0594	2.3	0.7684	2.0	0.0938	1.7	0.84	578.2	1.6	–0.1
13	2P17-35	789	707	1.12	0.0602	2.4	0.7699	2.1	0.0927	1.7	0.82	571.5	1.6	–1.4
14	2P17-37	523	542	0.96	0.0598	2.4	0.7686	2.1	0.0932	1.7	0.80	574.5	1.6	–0.8
15	2P17-40	345	374	0.92	0.0592	2.4	0.8151	2.2	0.0999	1.7	0.80	614.1	1.7	1.5
16	2P17-42	579	565	1.03	0.0597	2.2	0.8121	2.0	0.0986	1.7	0.88	606.4	1.6	0.5
17	2P17-43	367	390	0.94	0.0601	2.3	0.7788	2.1	0.0941	1.7	0.83	579.6	1.7	–0.9
18	2P17-44	518	531	0.97	0.0609	2.3	0.8149	2.1	0.0970	1.7	0.84	597.0	1.7	–1.3
19	2P17-46	463	469	0.99	0.0598	2.2	0.8195	2.0	0.0993	1.7	0.88	610.5	1.6	0.5
20	2P17-47	613	565	1.09	0.0597	2.2	0.8112	1.9	0.0985	1.7	0.88	605.7	1.6	0.4
21	2P17-50	511	525	0.97	0.0595	2.2	0.7998	2.0	0.0976	1.7	0.88	600.0	1.6	0.6
22	2P17-51	703	593	1.18	0.0597	2.2	0.7915	2.0	0.0963	1.7	0.88	592.4	1.6	0.1
23	2P17-52	537	519	1.03	0.0594	2.5	0.7788	2.2	0.0952	1.7	0.79	586.1	1.7	0.2
24	2P17-53	391	447	0.87	0.0599	2.3	0.8099	2.0	0.0980	1.7	0.86	602.7	1.6	0.1
25	2P17-58	778	746	1.04	0.0596	2.2	0.8011	2.0	0.0975	1.7	0.87	599.5	1.6	0.3
26	2P17-60	21	58	0.36	0.0607	3.0	0.8048	2.8	0.0963	1.8	0.65	592.4	1.7	–1.2
27	2P17-61	428	448	0.96	0.0600	2.3	0.7977	2.1	0.0965	1.7	0.84	593.7	1.6	–0.3
28	2P17-62	403	452	0.89	0.0593	2.3	0.7759	2.1	0.0949	1.7	0.84	584.4	1.7	0.2
29	2P17-66	700	638	1.10	0.0599	2.3	0.7794	2.1	0.0945	1.7	0.85	581.9	1.7	–0.6
30	2P17-67	346	463	0.75	0.0594	2.4	0.7660	2.1	0.0936	1.7	0.83	576.5	1.7	–0.2
31	2P17-68	1096	850	1.29	0.0601	2.2	0.8043	1.9	0.0972	1.7	0.91	597.7	1.6	–0.3
32	2P17-71	504	526	0.96	0.0594	2.4	0.7726	2.1	0.0943	1.7	0.83	580.8	1.7	–0.1
33	2P17-72	398	458	0.87	0.0598	2.3	0.8138	2.0	0.0988	1.7	0.86	607.3	1.6	0.4
34	2P17-74	149	243	0.61	0.0606	2.7	0.7859	2.5	0.0941	1.8	0.72	579.5	1.7	–1.6
35	2P17-76	459	525	0.88	0.0601	2.3	0.7974	2.0	0.0962	1.7	0.86	592.4	1.6	–0.5
36	2P17-80	382	405	0.94	0.0590	2.3	0.7789	2.0	0.0957	1.7	0.86	589.3	1.6	0.8
37	2P17-89	494	518	0.95	0.0597	2.3	0.7952	2.1	0.0966	1.7	0.84	594.3	1.6	0.0
38	2P17-90	577	565	1.02	0.0600	2.3	0.7930	2.0	0.0958	1.7	0.85	589.8	1.6	–0.5
39	2P17-95	778	688	1.13	0.0600	2.3	0.7885	2.0	0.0954	1.7	0.86	587.2	1.6	–0.5
40	2P17-97	724	640	1.13	0.0596	2.3	0.7882	2.0	0.0959	1.7	0.85	590.2	1.6	0.0
41	2P17-98	16	43	0.36	0.0587	5.0	0.7573	4.8	0.0936	2.1	0.43	576.6	2.0	0.7
42	2P17-100	724	788	0.92	0.0595	2.4	0.7672	2.2	0.0935	1.7	0.80	576.1	1.7	–0.3

Analytical results have been processed using Glitter program [92]; Rho, correlation coefficient of $^{207}Pb/^{235}U$ and $^{206}Pb/^{238}U$ ratio uncertainties; D—degree of discordance uncertainties are given at 2σ level.

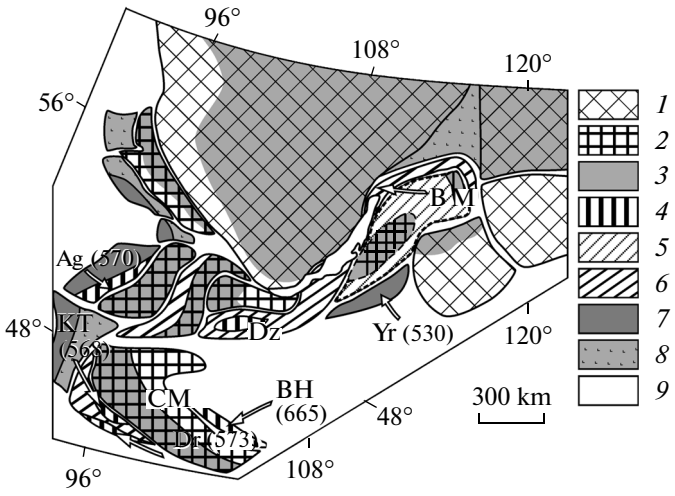

Fig. 10. Main tectonic elements, after [80], and age (Ma) of reference complexes at southern margin of Siberian Craton. (*1*) Craton; (*2*) microcontinent; (*3*) passive margins of craton and microcontinents; (*4*) ophiolite; (*5*) Late Neoproterozoic–Early Paleozoic tectonic collage (microcntinent with crust of transitional type); (*6*) middle Neoproterozoic island arc; (*7*) Cambrian island arc; (*8*) forearc and marginal basins; (*9*) post-Ordovician complexes. BH, Bayanhongor Zone; Dz, Dzhida Zone; Dr, Darib Zone; Ag, Agardag Zone; BM, Baikal–Muya Zone; KT, Khan-Taishir Zone; Yr, Yeravna Zone; CM, Central Mongolian Zone.

complexes, respectively) [14, 26, 81]. Thus, an extended paleoisland-arc system that actively developed 830–780 Ma ago has been reconstructed in the Sayan–Mongolian and Baikal–Muya segments of the Paleoasian ocean margin. The time interval from 780 to 650 Ma is the most obscure period in the history of the Baikal–Muya Belt.

Judging by the occurrence of eclogites pertaining to the North Muya Complex dated at 653 ± 21 Ma [58], subduction in the Baikal–Muya segment of the Paleoasian ocean margin resumed or continued by the end of Neoproterozoic. Granulite metamorphism spatially related to mafic magmatism and emplacement of adakitic intrusions about 590 Ma ago are the events that mark formation of the structure of the Baikal–Muya Belt, which is close to its recent pattern. Subduction zones continued to exist at that time in the Sayan–Mongolian domain. The belt of ophiolites dated at 570 Ma [9, 80, 88] extended to the west of the Darkhat–Sarkhoi paleoisland-arc system, as well as an island-arc belt with a peak of activity at 530 Ma ago [19, 39]. The epoch of suprasubduction volcanic activity dated at 530 Ma ago has also been reconstructed in the Uda–Vitim Fold System [13, 40, 41].

CONCLUSIONS

(1) Granulites and spatially related gabbroic plutons of the western Baikal–Muya Belt are intruded by granitoids with geochemical characteristics inherent to adakites. The deep-seated rocks have been transferred to the upper lithospheric levels instantaneously in geological comprehension. The granitoids sealed the heterogeneous structure no later than a few tens of millions of years after the formation of granulites.

(2) The structure of the western Baikal–Muya Belt is characterized by the juxtaposition of the Neoproterozoic granulite–charnockite complex; crystallization products of mantle-derived magmas at different depths (Tonky Mys, Slyudyanka, and Kurlinka complexes); and granitoids bearing attributes of mantle and crustal magma mixing. The geological situation is consistent with the formation of an asthenospheric window beneath the continental margin. This mechanism explains the heat supply necessary for the formation of granulites. The broken-off subducting plate led to decompression, giving rise to an outburst of mafic magmatism, tectonic movements oriented in various directions, transfer of granulites into the upper crust, emplacement of granitoids with adakitic geochemical characteristics, and filling of backarc basins with coarse-clastic molasse.

(3) No less than two large events in the late Neoproterozoic history of the Siberian margin of the Paleoasian ocean have been recorded in the structure of the western Baikal–Muya Belt. The heterogeneous belt (collage) with the participation of ophiolites and relics of the older Neoproterozoic island arc formed by the middle–late Neoproterozoic. Relics of the largest arc active since 830 Ma ago have been revealed not only in the Baikal–Muya Belt but also in the eastern Sayan and western Mongolia. About 600 Ma ago, the middle–late Neoproterozoic collage could have undergone transformation related to transition of convergent shortening settings to strike-slip faulting.

ACKNOWLEDGMENTS

We are grateful to A.B. Kotov and V.V. Yarmolyuk for constructive criticism,

G.E. Nekrasov for his consultations and assistance in processing the material, and A.V. Zabolotsky and E.V. Korostylev for cathodoluminescence study of zircon. This work was supported by the Russian Foundation in MIPT for Basic Research (project nos. 11-05-01052, 12-05-31246) and the Foundation for Development of Domestic Geology, it is contribution to IGCP#592 "Continental construction in Central Asia"

REFERENCES

1. Yu. V. Amelin, E. Yu. Rytsk, R. Sh. Krymsky, et al., "Vendian age of enderbite from a granulite complex of the Baikal–Muya ophiolite belt, northern Baikal Region," Dokl. Earth Sci. **371A** (3), 455–457 (2000).
2. V. A. Aristov, Yu. P. Katyukha, O. R. Minina, and S. V. Ruzhentsev, "Paleozoic stratigraphy and conodonts in the Uda–Vitim Fold System (Transbaikal

region)," in *Geodynamic Evolution of the Lithosphere of the Central Asian Foldbelt (from Ocean to Continents)*, Ed. by E. V. Sklyarov (Inst. Earth Crust, Irkutsk, 2010), Vol. 1, pp. 24–26 [in Russian].

3. V. A. Aristov, Yu. P. Katyukha, O. R. Minina, et al., "New data on Paleozoic stratigraphy of the Vitim Highland (western Transbaikal region)," Vestnik Voronezh State Univ., Ser. Geol., No. 2, 19–24 (2005).
4. V. G. Belichenko, *Caledonides of the Baikal Mountain Region* (Nauka, Novosibirsk, 1977) [in Russian].
5. N. A. Bozhko, V. G. Talitsky, A. B. Kirmasov, et al., "Structural and metamorphic criteria for subdivision of Upper Precambrian Sequences: a case of Kelyan–Irakinda Zone of the Baikal–Muya Belt)," Vestnik Moscow State Univ., Ser. 4, Geology, No. 4, 14–25 (1999).
6. A. N. Bulgatov, *Tektonotype of Baikalides* (Nauka, Novosibirsk, 1983) [in Russian].
7. Yu. P. Butov, *Paleozoic Sedimentary Rocks of the Sayan–Baikal Mountain Region* (Buryat Sci. Center, Siberian Branch, RAS, Ulan-Ude, 1996) [in Russian].
8. T. T. Vrublevskaya, A. A. Tsygankov, and D. A. Orsoev, "Contact reaction processesin the Nyurundukan ultramafic–mafic massif (northern Baikal region)," Geol. Geofiz. **44** (3), 207–223 (2003).
9. A. S. Gibsher, E. V. Khain, A. B. Kotov, et al., "Late Riphean age of the Khantaishir ophiolite complex in western Mongolia," Geol. Geofiz. **42** (8), 1179–1185 (2001).
10. D. P. Gladkochub, T. V. Donskaya, V. S. Fedorovsky, et al., "Ol'khon metamorphic terrane of the Baikal region: the Early Paleozoic composite of fragments at the Neoproterozoic active margin," Geol. Geofiz. **51** (5), 571–588 (2010).
11. I. V. Gordienko, "Geodynamic evolution of Late Baikalides and Paleozoides in fold framework of the southern Siberian Platform," Geol. Geofiz. **47** (1), 53–70 (2006).
12. I. V. Gordienko, A. N. Bulgatov, N. I. Lastochkin, and V. S. Sitnikova, "Composition and U–Pb isotopic age determinations (SHRIMP II) of the ophiolitic assemblage from the Shaman paleospreading zone and the conditions of its formation (North Transbaikalia)," Dokl. Earth Sci. **429A** (9), 1420–1425 (2009).
13. I. V. Gordienko, A. N. Bulgatov, S. V. Ruzhentsev, et al., "Evolution history of the Uda–Vitim island-arc system of the Transbaikal sector of the Paleoasian ocean in the Late Riphean–Paleozoic," Geol. Geofiz. **51** (5), 589–614 (2010).
14. E. I. Demonterova, A. V. Ivanov, L. Z. Reznitsky, et al., "Formation history of the Tuva–Mongolian Massif (western Hubsugul region, North Mongolia) based on U–Pb dating of detrital zircons from sandstone of the Darkhat Group by the LA–ICP–MS Method," Dokl. Earth Sci. **441** (1), 1498–1501 (2011).
15. T. V. Donskaya, D. P. Gladochub, A. M. Mazukabzov, et al., "Paleoproterozoic granitoids of the Chu and Kutim complexes (south of Siberian Craton): age, petrogenesis, and geodynamic nature," Geol. Geofiz. **54** (3), 371–389.
16. Yu. A. Zorin, E. V. Sklyarov, V. G. Belichenko, and A. M. Mazukabzov, "Mechanism of development of the island arc–backarc basin system and geodynamics of the Sayan–Baikal fold region in Late Riphean–Early Paleozoic," Geol. Geofiz. **50** (3), 209–226 (2009).
17. A. E. Izokh, Layered ultramafic–mafic associations as indicators of geodynamic settings, *Doctor Sci. (Geol.–Mineral.) Dissertation* (Novosibirsk, 1999).
18. A. E. Izokh, A. S. Gibsher, D. Z. Zhuravlev, and P. A. Balykin, "Sm–Nd dating of the ultramafic–mafic massifs of the eastern branch of the Baikal–Muya Ophiolite Belt," Dokl. Earth Sci. **360** (4), 525–529 (1998).
19. V. I. Kovalenko, V. V. Yarmolyuk, V. P. Kovach, et al., "Magmatism and geodynamics of Early Caledonian structures of the Central Asian Foldbelt (isotopic and geological data)," Geol. Geofiz. **44** (12), 1280–1293 (2003).
20. E. G. Konnikov, *Differentiated Ultramafic–Mafic Precambrian Complexes of the Transbaikal Region (Petrology and Ore Formation)* (Nauka, Novosibirsk, 1986) [in Russian].
21. E. G. Konnikov, "To problem of ophiolites in the Baikal–Muya Belt," Geol. Geofiz. **32** (3), 119–129 (1991).
22. E. G. Konnikov, A. S. Gibsher, A. E. Izokh, et al., "Late Proterozoic evolution of the northern segment of the Paleoasian ocean: new radiological, geological, and geochemical data," Geol. Geofiz. **35** (7/8), 152–168 (1994).
23. E. G. Konnikov, A. A. Tsygankov, and T. T. Vrublevskaya, *Baikal–Muya Volcanic–Plutonic Belt: Lithotectonic Complexes and Geodynamics* (GEOS, Moscow, 1999) [in Russian].
24. Yu. A. Kostitsyn and M. O. Anosova, "U–Pb age of extrusive rocks in the Uxichan Caldera, Sredinny Range, Kamchatka: application of laser ablation in dating young zircons," Geochem. Int. **51** (2), 155–163 (2013).
25. Yu. A. Kostitsyn, E. A. Belousova, and Ya. A. Bychkov, "Search for tracks of ancient crust in Kamchatka: U–Pb study of detrital zircons with method of laser ablation," in *Isotopic Systems and Time of Geological Processes* (Inst. Precambrian Geol. Geochron., St. Petersburg, 2009), Vol. 1, pp. 255–257 [in Russian].
26. A. B. Kuz'michev and A. N. Larionov, "Sarkhoi Group of the Eastern Sayan: Neoproterozoic (~770–800 Ma) Andean-type volcanic belt," Geol. Geofiz. **52** (7), 875–895 (2011).
27. A. B. Kuz'michev and A. N. Larionov, "Neoproterozoic island arcs of the Eastern Sayan: Duration of magmatic activity from results of zircon dating in volcaniclastic rocks," Geol. Geofiz. **54** (1), 45–57 (2013).
28. V. A. Makrygina, A. A. Koneva, and L. F. Piskunova, "Granulites of Nyurundukan Group in northern Baikal region," Dokl. Akad. Nauk SSSR **307** (1), 195–201 (1989).
29. V. A. Makrygina, E. G. Konnikov, L. A. Neimark, et al., "Age of granulite–charnockite complex in Nyurundukan Suite of northern Baikal region (paradox of radiochronology)," Doklady Russian Acad. Sci. **332** (4), 486–489 (1993).
30. O. R. Minina, Stratigraphy and miospore complexes of Upper Devonian sedimentary rocks in the Sayan–

Baikal mountain region, *Cand. Sci. (Geol.–Mineral.)* (Irkutsk: Inst. Earth Sci., 2003).

31. L. A. Neymark, A. M. Larin, A. A. Nemchin, et al., "Anorogenic nature of magmatism in the northern Baikal volcanic belt: evidence from geochemical, geochronological (U–Pb), and isotopic (Pb, Nd) data," Petrology **6** (2), 124–148 (1998).
32. G. E. Nekrasov, "Complexes in zones of crust–mantle discontinuity in continental and transitional structures and vertical accretion of the lithosphere," in *Vertical Accretion of the Earth's Crust: Factors and Mechanism*, Ed. by M. G. Leonov (Nauka, Moscow, 2002), pp. 237–267 [in Russian].
33. G. E. Nekrasov, N. V. Rodionov, N. G. Berezhnaya, et al., "U–Pb age of zircons from plagiogranite veins in migmatized amphibolites of the Shaman Range (Ikat–Bagdarin Zone, Vitim Highland, Transbaikal region)," Dokl. Earth Sci. **413** (2), 160–163 (2007).
34. A. V. Orlova, M. O. Anosova, and N. M. Revyako, "Geochronology and isotopic characteristics of matter sources of metamorphic rocks and granitoids in the Kichera Zone of the Baikal–Muya Belt," in *Proceedings of the Young Scientist Conferences, 4th Yanshin Lectures: Contemporary Problems of Geology* (GEOS, Moscow, 2011), pp. 144–146 [in Russian].
35. A. V. Orlova, M. O. Anosova, A. A. Fedotova, and Yu. A. Kostitsyn, "Crystallization age of zircon from enderbite–granulite association of northern Baikal region," in *Proceedings of 5th Russian Conference on Isotopic Geochronology: Geochronometric Isotopic Systems, Research Methods, and Chronology of Geological Processes* (IGEM RAS, Moscow, 2012), pp. 265–268 [in Russian].
36. L. M. Parfenov, N. A. Berzin, A. I. Khanchuk, et al., "Formation model of orogenic belts in central and northeastern Asia," Tikhookean. Geol. **22** (6), 7–41 (2003).
37. N. M. Revyako, Yu. A. Kostitsyn, and Ya. V. Bychkova, "Interaction between a mafic melt and host rocks during formation of the Kivakka layered intrusion, North Karelia," Petrology **20** (2), 101–119 (2012).
38. D. N. Remizov, E. V. Khain, and A. A. Fedotova, "Concept of asthenospheric windows in connection with structure and magmatism in the southern Siberia and Polar Urals," in *Geodynamic Evolution of the Lithosphere of the Central Asian Foldbelt (from Ocean to Continents)*, Ed. by E. V. Sklyarov (Inst. Earth Crust, Irkutsk, 2010), Vol. 2, pp. 69–72 [in Russian].
39. S. N. Rudnev, A. E. Izokh, V. P. Kovach, et al., "Age, composition, sources, and geodynamic environments of the origin of granitoids in the northern part of the Ozernaya Zone, western Mongolia: growth mechanisms of the Paleozoic continental crust," Petrology **17** (5), 439–475 (2009).
40. S. V. Ruzhentsev, O. R. Minina, V. A. Aristov, et al., "Geodynamics of the Eravna Zone (Uda–Vitim Fold System of the Transbaikal region): geological and geochronological data," Dokl. Earth Sci. **434** (3), 1168–1171 (2010).
41. S. V. Ruzhentsev, O. R. Minina, G. E. Nekrasov, et al., "The Baikal–Vitim Fold System: structure and geodynamic evolution," Geotectonics **46** (2), 87–110 (2012).
42. E. Yu. Rytsk, Yu. V. Amelin, N. G. Rizvanova, et al., "Age of rocks in the Baikal–Muya Foldbelt," Stratigr. Geol. Correlation **9** (4), 315–326 (2001).
43. E. Yu. Rytsk, V. P. Kovach, V. I. Kovalenko, and V. V. Yarmolyuk, "Structure and evolution of the continental crust in the Baikal Fold Region," Geotectonics **41** (6), 440–464 (2007).
44. E. Yu. Rytsk, V. P. Kovach, V. V. Yarmolyuk, et al., "Isotopic Structure and Evolution of the continental crust in the East Transbaikalian segment of the Central Asian Foldbelt," Geotectonics **45** (5), 349–377 (2011).
45. E. Yu. Rytsk, A. B. Kotov, V. P. Kovach, et al., "New data on geology and age of metamorphic complexes in the Kichera Zone of the Baikal–Muya Foldbelt," in *Geodynamic Evolution of the Lithosphere of the Central Asian Foldbelt (from Ocean to Continents)*, Ed. by E. V. Sklyarov (Inst. Earth Crust, Irkutsk, 2010), Vol. 2, pp. 55–56 [in Russian].
46. L. I. Salop, *Geology of the Baikal Mountain Region* (Nedra, Moscow, 1964) [in Russian].
47. S. R. Taylor and S. M. McLennan, *Continental Crust: Its Composition and Evolution* (Blackwell, Oxford, 1985; Mir, Moscow, 1988) [in Russian].
48. O. M. Turkina, A. D. Nozhkin, E. V. Bibikova, et al., "The Arzybei Terrane: a fragment of the Mesoproterozoic island-arc crust in the southwestern Framing of the Siberian Craton," Dokl. Earth Sci. **395** (2), 246–250 (2004).
49. A. A. Fedotova, A. V. Orlova, E. V. Khain, et al., "Western part of the Baikal–Muya Belt, deep slice of Neoproterozoic volcanic arc: geochemical and Sm–Nd isotopic data," in *Geodynamic Evolution of the Lithosphere of the Central Asian Foldbelt (from Ocean to Continents)*, Ed. by E. V. Sklyarov (Inst. Earth Crust, Irkutsk, 2013), pp. 252–254 [in Russian].
50. A. A. Fedotova and E. V. Khain, *Tectonics of the Southern Eastern Sayan and Its Position in the Ural–Mongolian Belt* (Nauchnyi mir, Moscow, 2002) [in Russian].
51. E. V. Khain, "Evolution of Paleoasian and Paleoatlantic (Iapetus) oceans in Neoproterozoic and Early Paleozoic," in *Geodynamic Evolution of the Lithosphere of the Central Asian Foldbelt (from Ocean to Continents)*, Ed. by E. V. Sklyarov (Inst. Earth Crust, Irkutsk, 2006), Issue 4, pp. 198–201 [in Russian].
52. V. E. Khain and E. V. Khain, "On some phenomena accompanying evolution of continental margins of the Andean–Cordilleran type: a case of southwestern and southern margin of the Siberian Platform," in *Tectonics of Asia, Program and Abstracts of Conference* (GEOS, Moscow, 1997), pp. 232–234 [in Russian].
53. E. V. Khain, "Accretion and obduction at the Ural–Kazakhstan and Siberian–Mongolian margins of the Paleoasian ocean as evidence for early stages of its closure (Neoproterozoic–Early Paleozoic)," in *Contemporary Status of Geoscience* (Faculty of Geology, Moscow State Univ., Moscow, 2011), pp. 1981–1985 [in Russian].
54. A. A. Tsygankov, *Magmatic Evolution of the Baikal–Muya Volcanic–Plutonic Belt in Late Precambrian* (Siberian Branch, RAS, Novosibirsk, 2005) [in Russian].

55. A. A. Tsygankov, "Mineralogy and thermometry of granulite–charnockite complex of northern Baikal region," Zapiski VMO **125** (6), 38–48 (1996).

56. A. A. Tsygankov, T. T. Vrublevskaya, and V. F. Posokhov, "Geochronology and genesis of hypersthene-bearing gneissic alaskite granites of the northern Baikal region," Geochem. Int. **38** (6), 542–551 (2000).

57. A. A. Tsygankov and E. G. Konnikov, "Geochemical types and geodynamic formation conditions of gabbroic complexes in the eastern branch of the Baikal–Muya ophiolite belt," Geol. Geofiz. **36** (1), 19–30 (1995).

58. V. S. Shatsky, E. Yagoutz, Yu. V. Ryboshlykov, et al., "Eclogites of the northern Muya Block: evidence for Vendian collision in the Baikal–Muya ophiolite belt," Dokl. Earth Sci. **351** (8), 1268–1270 (1996).

59. Y. V. Amelin, E. Y. Ritsk, and L. A. Neymark, "Effects of interaction between ultramafic tectonite and mafic magma on Nd–Pb–Sr isotopic systems in the Neoproterozoic Chaya massif, Baikal–Muya ophiolite belt," Earth Planet. Sci. Lett. **148**, 299–316 (1997).

60. E. Anders and N. Grevesse, "Abundances of elements: meteoritic and solar," Geochim. Cosmochim. Acta **53**, 197–214 (1989).

61. S. L. Baldwin, B. D. Monteleone, L. E. Webb, et al., "Pliocene eclogite exhumation at plate tectonic rates in eastern Papua New Guinea," Nature **431**, 263–267 (2004).

62. M. Brown, "A duality of thermal regimes is the distinctive characteristic of plate tectonics since the Neoarchean," Geology **34**, 961–964 (2006).

63. M. Brown, "Characteristic thermal regimes of plate tectonics and their metamorphic imprint throughout Earth history: when did Earth first adopt a plate tectonics mode of behavior?," Geol. Soc. Amer. Spec. Paper **440**, 97–128 (2008).

64. A. A. Bukharov, V. G. Glazunov, E. G. Konnikov, et al., *Early Precambrian of the Lake Baika Area. Guidebook for the Field Trip of the International Conference "Greenstone, Ophiolitic and Intracratonal Sialic Volcanic Belts of the Baikal Area*, Ed. by A. A. Bukharov (Institute of the Earth'S Crust, Irkutsk, 1990).

65. P. R. Castillo, "An overview of adakite petrogenesis," Chinese Sci. Bull. **51** (3), 257–268 (2006).

66. T. R. Charlton, "Postcollision extension in arc–continent collision zones, eastern Indonesia," Geology **19**, 28–31 (1991).

67. R. B. Cole and A. R. Basu, "Nd–Sr isotopic geochemistry and tectonics of ridge subduction and Middle Cenozoic volcanism in western California," GSA Bulletin **107** (2), 167–179 (1995).

68. M. J. Defant and P. Kepezhinskas, "Evidence suggests slab melting in arc magmas," EOS **82**, 62–70 (2001).

69. N. L. Dobretsov, E. G. Konnikov, and N. N. Dobretsov, "Precambrian ophiolite belts of southern Siberia, Russia, and their Metallogeny," Precambr. Res. **58**, 427–446 (1992).

70. M. S. Drummond and M. J. Defant, "A model for trondhjemite–tonalite–dacite genesis and crustal growth via slab melting: Archaean to modern comparisons," J. Geophys. Res. **95**, 21503–21521 (1990).

71. A. Fichtner, M. J. van Bergen, and M. De Wit, "Subduction of continental lithosphere in the Banda Sea region: combining evidence from full waveform tomography and isotope ratios," Earth Planet. Sci. Lett. **297**, 405–412 (2010).

72. R. Forsythe and E. Nelson, "Geological manifestations of ridge collision: evidence from the Golfo de Penas–Taitao Basin, southern Chile," Tectonics **4** (5), 477–495 (1985).

73. J. P. Haeussler, "A link between ridge subduction and gold mineralisation in southern Alaska," Geology **23**, 995–998 (1995).

74. R. A. Harris, "Peri-collisional extension the formation of Oman-type ophiolites in Banda Arc and Brooks Range," Geol. Society London Spec. Publ. **60**, 301–325 (1992).

75. E. G. Hill and S. L. Baldwin, "Exhumation of high-pressure metamorphic rocks during crustal extension in the D'Entrecasteoux region, Papua New Guinea," J. Metamorph. Geol. **11**, 261–277 (1993).

76. D. J. Ellis, "Origin and evolution of granulites in normal and thickened crusts," Geology **15**, 167–170 (1987).

77. A. Ishikawa, Y. Kaneko, A. Kadarusman, and O. Tsutomu, "Multiple generations of forearc mafic–ultramafic rocks in the Timor–Tanimbar ophiolite, eastern Indonesia," Gondwana Res. **11**, 200–217 (2007).

78. Y. Kaneko, S. Maruyama, A. Kadarusman, et al., "On-going orogeny in the outer-arc of the Timor–Tanimbar region, eastern Indonesia," Gondwana Res. **11**, 218–233 (2007).

79. E. V. Khain, E. V. Bibikova, A. Kröner, et al., "The most ancient ophiolite of the Central Asian Fold Belt: U–Pb and Pb–Pb zircon ages for the Dunzhugur Complex, Eastern Sayan, Siberia, and geodynamic implications," Earth Planet. Sci. Lett. **199**, 311–325 (2002).

80. E. V. Khain, E. V. Bibikova, E. B. Salnikova, et al., "The Palaeo-Asian ocean in the Neoproterozoic and Early Palaeozoic: new geochronologic data and palaeotectonic reconstructions," Precambr. Res. **122**, 329–358 (2003).

81. V. V. Khomentovsky and A. S. Gibsher, "The Neoproterozoic–Lower Cambrian in northern Gobi-Altay, western Mongolia: regional setting, lithostratigraphy and biostratigraphy," Geol. Mag. **133** (4), 371–390 (1996).

82. Y. Lagabrielle, C. Guivel, R. Maury, et al., "Magmatic–tectonic effects of high thermal regime at the site of active ridge subduction: the Chile triple junction model," Tectonophysics **326**, 255–268 (2000).

83. K. Liu, A. Levander, Y. Zhai, et al., "Asthenospheric flow and lithospheric evolution near the Mendocino triple junction," Earth Planet. Sci. Lett. **323/324**, 60–71 (2012).

84. K. R. Ludwig, *Isoplot 3.0. A Geochronological Toolkit for Microsoft Excel* (Geochronology Center Spec. Publ., Berkeley, 2003), No. 4.

85. H. Martin, R. H. Smithies, R. Rapp, et al., "An overview of adakite, tonalite–trondhjemite–granodiorite (TTG), and sanukitoid: relationships and some implications for crustal evolution," Lithos **79**, 1–24 (2005).

86. H. Martin, "The adakitic magmas: modern analogues of Archaean granitoids," Lithos **46** (3), 411–429 (1999).

87. L. M. Parfenov, G. Badarch, N. A. Berzin, et al., "Summary of major metallogenic belts in northeast Asia," U.S. Geol. Survey Prof. Paper **1765**, 17–33 (2010).

88. J. A. Pfänder, K.-P. Jochum, I. Kozakov, et al., "Coupled evolution of back-Arc and island arc-like mafic crust in the Late Neoproterozoic Agardagh Tes-Chem ophiolite, central Asia: evidence from trace element and Sr–Nd–Pb isotope data," Contrib. Mineral. Petrol. **143**, 154–174 (2002).

89. A. A. Razumovskiy, E. V. Khain, and A. A. Fedotova, "Correlation of the Neoproterozoic events at the Siberian margin of the paleo-Asian ocean: new structural evidences from the Tonky Mys Peninsula, the North Baikal area," *33rd International Geological Congress. ASI-06 Pre-Mesozoic Accretionary Tectonics in Central Asia* (Oslo, 2008) ASI06326.

90. A. Schoonmaker and W. S. F. Kidd, "Evidence for a ridge subduction event in the Ordovician rocks of North-Central Maine," Geol. Soc. Amer. Bull. **118** (7/8), 897–912 (2006).

91. U. S. Brink, S. Marshak, and J.-L. Granja Bruna, "Bivergent thrust wedges surrounding oceanic island arcs: insight from observations and sandbox Models of the northeastern Caribbean Plate," Geol. Soc. Amer. Bull. **121** (11/12), 1522–1536 (2009).

92. E. van Achterbergh, C. G. Ryanm, and W. L. Griffin, "GLITTER: On-line interactive data reduction for the laser ablation ICP-MS microprobe," in *Proceedings of the 9th V.M. Goldschmidt Conference* (Cambridge, Massachusetts, 1999).

93. J.-F. Xu, R. Shinjo, M. J. Defant, et al., "Origin of Mesozoic adakitic intrusive rocks in the Ningzhen area of East China: partial melting of delaminated Lower Continental Crust"? Geology **30** (12), 1111–1114 (2002).

Reviewers: V.V. Yarmolyuk and A.B. Kotov

Translated by V. Popov